Design and Study of Additively Manufactured Terahertz Antennas and Baluns

by

Afahaene Edet Uya

Submitted in Partial Fulfillment of the Requirements

for the Degree of

Master of Science

in the

Electrical and Computer Engineering

Program

YOUNGSTOWN STATE UNIVERSITY

December 2023

Design and Study of Additively Manufactured Terahertz Antennas and Baluns

Afahaene Edet Uya

I hereby release this **thesis** to the public. I understand that this **thesis** will be made available from the OhioLINK ETD Center and the Maag Library Circulation Desk for public access. I also authorize the University or other individuals to make copies of this thesis as needed for scholarly research.

Signature:

_____

Afahaene Edet Uya, Student Date

Approvals:

_____

Vamsi Borra, PhD, Thesis Advisor Date

_____

Srikanth Itapu, PhD, Committee Member Date

_____

Frank X. Li, PhD, Committee Member Date

_____

Pedro Cortes, PhD, Committee Member Date

_____

Salvatore A. Sanders, PhD, Dean, College of Graduate Studies Date

ACKNOWLEDGEMENT

I would like to thank Dr. Vamsi Borra for the guidance and wisdom he provided. His expertise and patience have greatly enriched my academic journey. The invaluable advice and support I received at every stage of my research were pivotal to its completion.

I would also like to thank the members of my committee, Dr. Srikanth Itapu, Dr. Frank Li, and Dr. Pedro Cortes, for their valuable insights and suggestions. Their contributions were crucial in shaping the direction and execution of my research.

I am also grateful for the unwavering support of the staff at the Electrical Engineering department and STEM faculty in Youngstown State University. Their assistance and provision of excellent facilities were integral to my work.

A special note of thanks to my fellow researchers and friends Kwame, Brendan, Jairo, Yogesh, Uttam, Suman, Khaled, Sanjee and Bhawana. The environment of collaboration and friendship we shared was a source of joy and motivation throughout this journey.

My family, particularly my mother and father, have been a constant source of love and encouragement. Their understanding and emotional support have been the cornerstone of my resilience and commitment.

I would also like to acknowledge the financial support from the U.S Air Force Research Laboratories and express my gratitude to the research team in the Electrical and Computer engineering department at Cleveland State University, led by Dr. Lili Dong, for their role in facilitating aspects of my research.

This accomplishment is not just a reflection of my efforts but is also a testament to the unwavering support and contributions of everyone mentioned above, to whom I am deeply thankful.

ABSTRACT

Design and Study of Additively Manufactured Terahertz Antennas and Baluns

by

Afahaene Edet Uya

This thesis investigates a novel terahertz (THz) antenna for advanced THz communications and a performance analysis of a balun design fabricated using two additive manufacturing methods and a traditional method. It proposes a THz antenna with a peak gain of 0.38 dB at 0.125 THz, suitable for MIMO systems due to its multi-directional radiation and broad impedance bandwidth. The study also compares PCB with screen-printing and aerosol jet printing manufacturing techniques for balun production, highlighting the performance of the design when printed on flexible and rigid FR-4 substrates.

Significant findings include the critical role of substrate material on the balun's RF performance, with different materials affecting bandwidth and efficiency. The research presented contributes to the THz field by offering insights into design and manufacturing impacts on high-frequency communication devices, supporting the development of more efficient THz communication technologies.

Table of Contents

Chapter 5: Conclusions and Future Work

List of Figures:

Chapter 1: Introduction

1.1 Background and Motivation.

Lately, there's been a big push for better, smaller, and more flexible electronic devices. People need quicker ways to communicate and stronger devices for detecting things, which has made the terahertz (THz) frequencies more important. These frequencies could be used for fast internet, checking health in safer ways, and keeping data secure. But, making antennas that work at these high frequencies is tricky because as we go higher in frequencies, the size of the components reduces. This makes the usual ways of producing them hard to implement.

Aerosol Jet Printing (AJP) emerges as a compelling technique in the fabrication of electronic devices, particularly in the micro and nano-scale realm. It offers significant advantages over traditional manufacturing methods because it can handle a wide variety of materials and is compatible with both rigid and flexible substrates. These capabilities could be leveraged to produce next-generation antennas, particularly those operating in the elusive terahertz regime.

Furthermore, the integrity of signal transmission and reception in antennas is significantly determined by their feeding networks. Baluns, being crucial components in these networks, serve as a bridge between balanced and unbalanced systems, ensuring efficient signal propagation and minimal reflection. The design of baluns, especially when considering novel substrates introduced by techniques such as AJP, poses a new set of challenges and opportunities.

1.2 Objective of the Study.

The primary objectives of this research are:

1. To design and develop a terahertz antenna using aerosol jet-printing (AJP) technique, assessing its performance and potential advantages over traditionally fabricated counterparts.

2. Investigate the design considerations, development, and performance analysis of baluns on both rigid and flexible substrates. The focus would be on understanding the unique challenges and opportunities presented by these substrates in the context of antenna feeding networks.

1.3 Research Scope and Limitations.

This research will primarily focus on the THz frequency range for antenna design, considering the increasing interest and applicability in this range. While AJP offers a broad array of substrate choices, the study will predominantly revolve around popular rigid substrates like silicon and flexible ones such as polyimide due to their widespread usage and potential for real-world applications.

The balun design will be approached considering commonly used architectures, but the focus will be on how these designs perform and may be optimized for AJP fabricated structures on the selected substrates.

1.4 Thesis Structure.

Chapter 2 will delve into the fundamentals of terahertz antennas, highlighting the challenges and current solutions in the design and fabrication domain. We will briefly talk about baluns, their evolution, and different types. We will also introduce Aerosol Jet Printing, its mechanism, advantages, and potential in electronic device fabrication.

Chapter 3 will be centered on the design considerations, development process, and testing of the terahertz antenna fabricated using AJP. This will involve simulation and fabrication phases to gauge the antenna's performance.

Chapter 4 will provide a deep dive into the world of baluns, their significance in antenna systems, and the challenges posed by different substrates. The chapter will culminate in the design, fabrication, and analysis of baluns using AJP on both rigid and flexible substrates.

Chapter 5 will synthesize the findings from the research, discuss the implications, potential applications, and future work directions in the domain.

Chapter 2: Literature Review

2.1 Introduction to Terahertz Technology and Its Applications.

Terahertz (THz) technology is gaining momentum among global researchers, thanks to its promising uses in fields such as advanced radars, imaging systems, detection, security checks, and fast communication methods [1]-[10]. Antennas are fundamental in driving these innovations. A variety of THz antennas like horn types, slotted waveguides, reflectors, and dielectric lenses have emerged [11]-[28]. Particularly, dielectric lens antennas stand out because of their simple structure, superior gain, broad frequency range, lack of conductor-related losses, and their capability for circular polarization [19]-[25].

The spectrum of THz technology, ranging from 0.1 THz to 10 THz, has become a focal point due to its diverse applications in imaging, spectroscopy, wireless data transfers, and safety systems. Crafting effective terahertz antennas is essential for propelling these applications forward. Yet, the creation and design of terahertz antennas come with their set of challenges, like picking the right materials, ensuring accurate fabrication, and amalgamating with other elements. Microstrip antennas, known for their slim design, lightness, and compatibility with other electronic parts, are considered promising for terahertz applications.

Traditional methods of fabricating microstrip antennas, like photolithography or electron-beam lithography, might be costly, lengthy, and might not deliver the sharpness needed for tiny terahertz antennas. Hence, alternative methods promising better accuracy and simpler processes are gaining attention.

Techniques like fused deposition modeling (FDM), digital light processing (DLP), and polymer jetting (PolyJet) are popular for crafting components in the millimeter-wave and THz range, including antennas [29]-[31], waveguides [32]-[33], and THz detectors [34]-[35]. Among these, DLP is often chosen over FDM and PolyJet due to its capacity to produce high-definition 3D constructs and a broad choice of printable materials [36].

Terahertz technology is advancing quickly, and making antennas that work well at these high frequencies is important. With Aerosol Jet Printing (AJP), making these detailed antennas becomes easier. AJP is a precise way to print complex parts and circuits right where they're needed, which is great for the tiny and precise details required in THz antennas.

AJP is valuable because it can handle many different materials and create complex shapes that are just right for THz devices. This printing technique is not only faster but also wastes less material than older ways of making things. With AJP, we can make THz components that are essential for the future of fast wireless communications more quickly and efficiently.

2.2 Aerosol Jet Printing (AJP) in Electronics and Antenna Fabrication.

3D printing, or additive manufacturing, is now a cornerstone in contemporary 3D creation techniques, recognized for its quick design testing and budget-friendly creation [37]. It also offers a variety of materials suitable for 3D printing.

Aerosol Jet Printing (AJP) is a 3D printing method that directly prints functional materials (small droplets between 2 - 5 μm in size) with great precision and detail, making it ideal for creating terahertz antennas [38]. This approach allows the creation of intricate designs with little material wastage, and there's no need for masks or etching, which are typically used in older methods. In this study, we detail the making, building, and testing of a microstrip THz antenna measuring 3mm x 2mm. We used Optomec's AJP technology to print the antenna design. The antenna is made to work within the terahertz frequency spectrum, keeping in mind the insulation properties of its base material and the conducting qualities of the printed metal layer.

2.3 Traditional and Modern Balun Designs.

At the heart of modern wireless communication systems is the balun. This essential electrical device serves to interconnect balanced and unbalanced lines, facilitating undistorted and seamless signal transmissions across diverse electronic and communication platforms.

Definition and Role:

- Balun: Stemming from the terms "balanced" and "unbalanced", this device acts as a bridge between these two types of lines, preserving their unique impedances. Although it has the potential to transform impedances, it isn't always required to do so. Various configurations exist, some employing magnetic coupling, while others do not. Importantly, common-mode chokes, known to counteract common-mode signals, function in similar capacities as baluns.

Delineating Lines:

- Balanced Line: Comprises two conductors, each carrying equal but opposite potentials. This setup is critical for efficient signal conveyance.
- Unbalanced Line: These are typically represented by microstrip and coaxial cables which have conductors of differing dimensions, underscoring the necessity for an intermediary for optimal performance.

The Evolution and Diversity of Baluns:

Over time, baluns have undergone significant design evolution, presenting a variety of types:

1. Classical Transformer Type Balun: Features two distinct windings encircling a core. Functioning on the principle of magnetic induction, its efficiency hinges on the winding ratio and the strength of magnetic coupling.
2. Auto-transformer Type Balun: Comprising interconnected coils, this type facilitates a pathway for DC currents, especially beneficial for specific antenna types.

3. Transmission-line Transformer Type Balun: Designed to ensure uniform current distribution on both output sides, this combines both magnetic and electromagnetic coupling.

4. Delay-Line Type Balun: Employs transmission lines of predetermined lengths, making it especially apt for designated frequencies.

5. Marchand Balun: Recognized for its intricate design and adaptability, this modern incarnation distinctly employs transmission line coupling principles, reminiscent of those observed in coupled-line devices. The configuration encompasses two closely intertwined transmission lines wrapped around a mutual conductor or core. Upon receiving an unbalanced input, the signal divides, and traverses both lines. Intriguingly, one of these lines inverses the signal due to the balun's unique structure. As these signals come together at the terminal, a harmonized, balanced output is generated.

Key Performance Metrics and Research Trajectories:

Given their centrality in modern communication, baluns are subject to intense research to enhance their performance, especially in the domains of signal balance and isolation. Two primary performance metrics are return loss, which measures reflection characteristics, and insertion loss, which quantifies the attenuation of signal power.

$$RL\ (\mathrm{dB}) = 10 \log_{10} (P_i/P_r)$$

where RL (dB) is the return loss in dB, P_i is the incident power and P_r is the reflected power [39].

$$IL\ (\mathrm{dB}) = 10 \log_{10} (P_T/P_R)$$

where *IL* (dB) is the insertion loss in dB, P_T is the power transmitted to the load before insertion and P_R is the power received by the load after insertion [40].

Challenges and Innovations:

Despite these advancements, there remain obstacles, notably the quest for cost-effective production and fabrication of complex designs. In this context, additive manufacturing techniques, spanning 3D printing, and screen-printing, present themselves as promising solutions, blending precision with cost-efficacy.

Study Highlights:

In this research, we delve deep into the intricacies of a microstrip dual-band balun, gauging its efficacy across diverse additive manufacturing techniques and substrate materials. The critical findings of this study were:

1. Manufacturing Process and Frequency Ranges: The operational frequency ranges of baluns showcased a distinct pattern based on their manufacturing technique:

- Screen-printing on flexible substrate: Demonstrated optimal performance in the frequency brackets of 3.1285 GHz - 3.2317 GHz and 8.8960 GHz - 9.1143 GHz.
- PCB fabrication: Emerged superior in the range of 7.06 GHz – 7.45 GHz and 10.22 GHz – 10.99 GHz.
- Aerosol 3D jet printing: Displayed unparalleled efficacy between 2.92 GHz – 3.59 GHz and 14.3 GHz – 18.6 GHz.

2. Additive Manufacturing's Potential: The study underscores that the choice of a manufacturing process isn't merely about production ease or cost. It strategically influences the operational frequency and, by extension, the specific applications, and requirements of the communication systems these baluns integrate into.

3. Performance Analysis with Ansys Electronics Desktop 2022 R2: This state-of-the-art design and simulation tool was employed to meticulously examine the balun design that spanned screen-printing, PCB fabrication, and aerosol 3D jet printing. Each printed design was meticulously scrutinized, particularly in terms of signal isolation and balance attributes.

Conclusion and Future Outlook:

The microstrip dual-band balun's compact yet efficient design sets it apart from its conventional counterparts. This investigation not only confirms the transformative potential of additive manufacturing in the arena of balun production but also charts a promising trajectory for wireless communication technology's future.

Baluns, having transitioned from their rudimentary designs to sophisticated configurations, have established themselves as indispensable in the ever-evolving landscape of communication systems. Whether they're ensuring impedance compatibility, preventing unintended radiation, or adapting to the diverse needs of state-of-the-art communication infrastructures, baluns underscore the importance of continued research and innovation in our hyper-connected era.

2.4 Impact of Substrate Types on Antenna and Balun Performance.

Selecting the appropriate substrate material is a critical decision in design that influences not only the electrical, mechanical, and environmental performance but also the cost-effectiveness of the final product. Air is often chosen as a substrate for baluns due to its excellent efficiency, superior gain, and wide impedance bandwidth, along with minimal surface wave loss.

For dielectric substrates, those with a low loss tangent are preferable because they minimize the conversion of electrical energy into heat, thereby improving balun efficiency. It's important to note that the dielectric constant of the material impacts the size and performance of the balun; a higher dielectric constant reduces the size but also decreases bandwidth and directivity and increases the loss due to surface waves. High dielectric constants also require more precise manufacturing [41].

Ensuring uniformity in dielectric constant is vital for the dependability of baluns. Therefore, analyzing and optimizing production techniques, such as etching precision, material thickness, and feed point placement, is essential. Substrate materials may react differently to temperature changes, which can affect their properties. For instance, materials like Teflon/fiberglass have been shown to exhibit variations in their dielectric properties under different temperature conditions, an issue particularly relevant in aerospace contexts [42].

The diversity of substrates available in the market each comes with its own set of fabrication requirements. It is essential to understand these specifications, which can be found in existing scholarly literature and manufacturers' guidelines [43]. Recent studies have explored novel fabrication methods, like using conductive inks for screen printing directly onto substrates [44] and advancements in inkjet printing technology [45].

Lastly, while both dielectric permittivity and loss tangent typically increase with temperature, in the vacuum of space, the phenomenon of moisture outgassing can cause these values to decrease. This is a crucial consideration for space-bound applications.

Dielectric Substances

Dielectric substrates employed in the creation of planar antennas and baluns can be categorized into several groups. These include plastics, notably fluoropolymers such as PTFE (often known as Teflon) and Rexolite 1422, which is a form of cross-linked polystyrene. There are also ceramics, like alumina (Al2O3) and silicon nitride (Si3N4), alongside glasses, with E-Glass being a common component in many Teflon-fiberglass microwave substrates.

In specific commercial contexts, a flat antenna might be encased in an injection-molded protective cover, known as a radome. It's crucial to consider the dielectric qualities of the resins in this design. Ideally, these resins would exhibit minimal moisture absorption attributes to ensure that both the resonance frequency and loss properties remain stable in varying humidity conditions.

Materials can be broadly categorized as either hydrophobic or hydrophilic. The former, hydrophobic materials, repel water and hold negligible amounts. An example of this behavior can be seen with water droplets forming beads on wax paper due to the wax's water-repellent nature. In contrast, hydrophilic materials are drawn to water, absorbing it readily.

For those designing planar antennas, water presents unique challenges. Specifically, its relative dielectric permittivity shifts from around 90 at 1.5°C to roughly 80 at 25°C within the frequency range of about 5-10 GHz. At 10 GHz, this permittivity drops swiftly, with the dielectric loss reaching a peak and then declining. The most significant loss in this context happens slightly above the freezing point. When temperatures drop further, causing water to solidify, its dielectric permittivity shifts to a value near three, and the associated dielectric loss becomes minimal [46].

Table 1, enumerates several substrate materials typically employed in planar antenna designs, detailing standard relative dielectric permittivity and loss tangent values.

Table 1 *Common dielectric substrate material properties*

Material	**Dielectric permittivity**	**Loss tangent (tan *δ*)**
Teflon (PTFE)	2.1	0.0005
FR-4	4.1	0.02
Alumina (99.5 %)	9.8	0.0003

Plastics

- *Teflon (PTFE):* While Teflon boasts favorable electrical properties, its softness makes it unsuitable for many space applications due to its tendency for "cold flow" deformation [47].
- *Rexolite 1422:* This early-used material in planar transmission line design is ideal for space applications due to its mechanical properties [48, 49]. It's stable up to 100 GHz, and its fiberglass-reinforced version, Rexolite 2200, is more rigid.
- *Noryl:* A suitable choice for many commercial microwave setups due to its cost-effectiveness and low loss. However, its softness and low melting point can pose challenges.

Ceramics

- *Alumina (Al2O3):* Offers good microwave attributes but can be brittle and challenging to work with. It's beneficial in aerospace applications where heat dissipation is crucial.
    - *Corundum:* Alumina's crystalline form which can be powdered to produce a material with isotropic dielectric permittivity.
    - *Sintered Alumina:* Created by heating alumina powder, its porosity affects its dielectric permittivity [50]. The sintering process involves the fusion of particles, with two types of grain growth observed - normal and abnormal. The size of the grains can impact the material's loss tangent [51].
    - *Doping:* To enhance sintering, dopants such as magnesium oxide or titanium dioxide are sometimes added. These can significantly influence the material's properties [52].

Glass Transition Temperature (Tg)

- *Polymers:* Used in microstrip antenna substrates and radomes. The distinction between plastic and rubber is based on the position of the glass transition temperature. If it's above room temperature, the material is classified as plastic, and if below, it's considered rubber [53].
    - *Reinforcements:* Rubber can be reinforced with carbon black for enhanced structural integrity, except in the case of silicone rubber, which incorporates fumed silica particles [54].

Composite Dielectric Materials:

Dielectric materials are sometimes mixed to create composite materials, where each retains its distinct properties. Several microwave substrates available commercially combine multiple dielectrics, such as Teflon with fiberglass or epoxy with fiberglass. Rexolite 1422 is pure cross-linked polystyrene, but there's also a version with fiberglass: Rexolite 2200. Ultem (Polyetherimide) can be obtained either in its pure form or with varied percentages of fiberglass reinforcement [55].

Flame Retardant 4 (FR-4):

FR4 stands out as a prime substrate material in the electronics domain, esteemed for its unique blend of mechanical robustness, electrical insulation, and thermal stability. This budget-friendly material is primarily constructed from woven fiberglass sheets infused with thermoset epoxy. Such a composition bestows upon FR4 a commendable dielectric constant, making it apt for RF (radio frequency) applications, particularly in the

frequency realm up to 10 GHz. The dielectric permittivity of FR4 is contingent on the proportion of its core components, varying from 3.9 to 4.6 [56]. While it proves efficient for various wireless applications, caution is advised for uses beyond 10 GHz due to potential inconsistencies in its dielectric permittivity.

In addition to its base form, FR4 manifests in diverse variations tailored for specific needs, including high-performance FR4, resilient to elevated temperatures, and halogen-free FR4, advocating for environmentally conscious disposal. Its flame-resistant attribute, a nod to its very name, underscores its value in safety-critical projects. The broad spectrum of its applications encompasses everything from conventional printed circuit boards (PCBs) to sophisticated electronic components like antennas and high-frequency transmission lines. As we usher in new technological eras, FR4's adaptability heralds its role in avant-garde areas like wearables and IoT devices. Engineers and designers, presented with the plethora of FR4 variants, are empowered to cherry-pick the most fitting version to meet their distinct project prerequisites. It's pivotal to note that FR4 undergoes a singular, irreversible chemical transformation upon heating, which distinguishes it from thermoplastics like Noryl. The latter, when exposed to heat, can melt, and be remolded without permanent chemical alterations, although recurrent reprocessing may compromise its integrity. The dual nature of FR4, both in its adaptability and chemical makeup, accentuates its pivotal position in the continually evolving electronic landscape.

It is crucial to understand the dielectric permittivity of a substrate as it represents how quickly a material can respond and line up its tiny charged parts when an electric field is applied to it. This means that we need to pay close attention to how the material is made up, especially looking at how much of each material is mixed to develop the substrate. This mix has a big impact on figuring out the material's actual dielectric permittivity.

In summary, this text provides an in-depth exploration of various dielectric materials, their characteristics, and their applications in antenna designs and other microwave applications.

Chapter 3: Terahertz Antenna Design Fabrication

3.1 Introduction.

This chapter focuses on the fabrication of the THz antenna, crucial for next-gen high-speed wireless communication. It covers the design using the simulation software, materials required for the fabrication process, and the challenges faced.

3.2 Design Principles for Terahertz Antennas.

THz antennas, operating between 0.1 and 10 THz, must be precision-engineered due to their compact size and the unique propagation characteristics of THz waves. Design factors considered include:

1. *Minimization:* THz antennas are significantly smaller, demanding exact manufacturing methods like photolithography.

2. *Materials:* Metals for conductive parts and low-loss dielectrics are chosen to reduce energy loss.

3. *Bandwidth:* Designs aim for wideband operation to utilize the THz range's vast bandwidth.

4. *Integration:* Antennas are designed for integration with system components, requiring a holistic design approach.

5. *Efficiency:* High efficiency and gain are vital to combat the inherent path loss at THz frequencies.

6. *Beamforming:* Antennas often feature beamforming for directional control.

7. *Thermal Management:* Design must include heat dissipation strategies.

8. *Impedance Matching:* Ensuring power transfer efficiency involves impedance matching, described by: $Z = R + jX$.

9. *Polarization:* Control of the radiated wave's polarization is critical, influencing the antenna design.

Antenna dimensions are dictated by the wavelength (λ), derived from the speed of light (c) and the operational frequency (f):

$$\lambda = \frac{c}{f}$$

For dipoles, the length (L) is usually $L = \frac{\lambda}{2}$. For patch antennas, the width (W) and length (L) are calculated considering the effective dielectric constant ($\mathcal{E}_r^{eff}$), influenced by the substrate's material properties:

$$W = \frac{c}{2f\sqrt{\mathcal{E}_r^{eff}}}$$

$$L < \frac{\lambda}{2}$$

where (L) is adjusted for fringing fields. Precision in dimensioning is critical as THz antennas are highly sensitive to size variations.

3.3 Ansys HFSS Simulation Software.

Ansys HFSS is a state-of-the-art electromagnetic simulation software that stands out for its prowess in high-frequency structure simulation. Rooted in the finite element method, HFSS delivers a comprehensive toolset tailored for 3D full-wave electromagnetic field simulation. With its robust capabilities, this software excels in addressing complex electromagnetic challenges spanning from antennas, passive RF components, to intricate microwave circuits. Engineers and researchers across various sectors, including aerospace, telecommunications, and electronics, harness the potential of Ansys HFSS to design, analyze, and optimize high-frequency components. Its meticulous simulations empower users to foresee the real-world performance of their designs, mitigating risks

and refining efficiency. Additionally, with the escalating demands of wireless technology and 5G integration, HFSS is at the forefront, providing invaluable insights into electromagnetic interference, signal integrity, and radiation patterns. Through the interactive and intuitive interface of Ansys HFSS, professionals are equipped to usher in innovative solutions while ensuring optimal electromagnetic performance [57].

3.4 Antenna Design and Simulation.

This study showcases a terahertz microstrip antenna layout of 3mm x 2mm, and we employed the Ansys HFSS tool for our simulation activities. We've used flexible FR4 material to create the microstrip pathways, with a dielectric constant (εr) of 3.55. The FR4 material is chosen for its efficiency in terahertz tasks due to minimal signal losses at higher ranges. Its flexible nature broadens the usability of the antenna, fitting various forms and base surfaces.

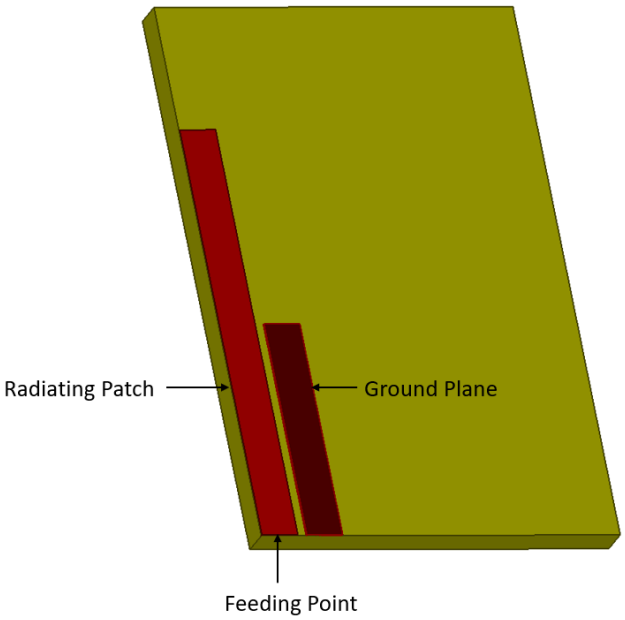

Figure 1. Simulated Design

The antenna layout features an emitting patch, sized 2.3 mm x 0.2 mm, and a ground section, sized 1.2 mm x 0.2 mm, positioned on the FR4 platform. The flexible base material has a depth of 0.1 mm. Precise measurements for the patch and transmission line are crucial for achieving peak performance at the aimed terahertz range. The Ansys HFSS tool assists in refining design elements like frequency resonance, bandwidth, radiation direction, and matching impedance.

The antenna's function hinges on the excitation of the primary mode at the chosen terahertz range, projecting energy from the patch outwards. The ground section boosts the radiation effectiveness and trims down losses. The flexibility of the FR4 allows for Ansys HFSS to gauge the antenna's adaptability under different bend scenarios, making it a good fit for wearable tech, bendable communication tools, and adaptive radars. The antenna simulation is displayed in Figure 1.

3.5 Overview of Fabrication Process using Aerosol Jet Printing (AJP).

The design was produced using the Optomec Aerosol Jet 200 printer, renowned for its precision in printing features between approximately 10 to 200 microns and a maximum printing speed of 100mm/sec. This equipment is adept at creating complex electronic components, such as terahertz antennas, and depositing them on heat-resistant substrates.

The production begins with creating conductive nanoparticle inks, which are then adjusted for the ideal viscosity and flow dynamics. The Optomec AJP device utilizes a nozzle (100um) to project a gas-guided stream of ultrasonically aerosolized ink onto the surface of an FR4 substrate. Fine-tuning the deposition parameters, including nitrogen gas pressure and the printing velocity, achieves a consistent, high-definition pattern deposition critical for optimal antenna operation.

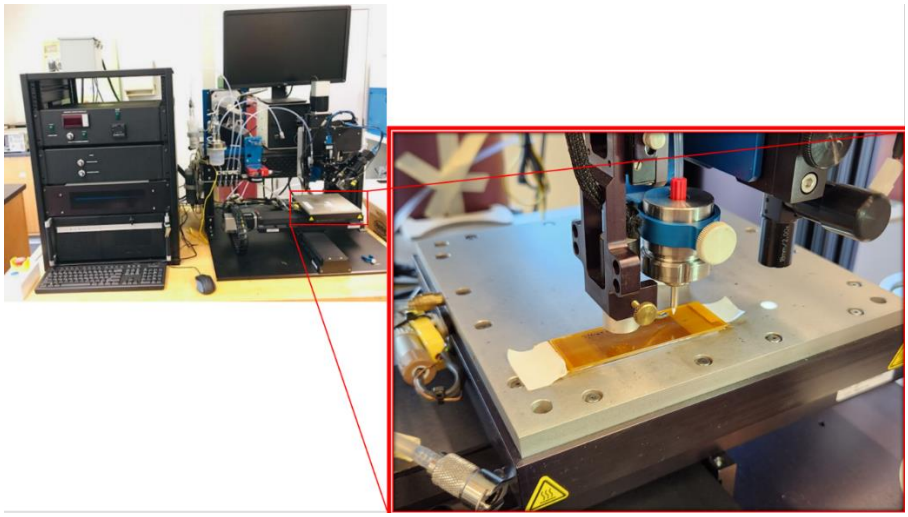

Figure 2. Optomec AJP Printer

Figure 2 captures the Optomec printer in action, highlighting its print stage and print head in the close-up inset. Post-printing procedures, like curing and sintering, were done to ensure electrical flow and adhesion. Figure 3 captures the curing oven used for sintering the fabricated design.

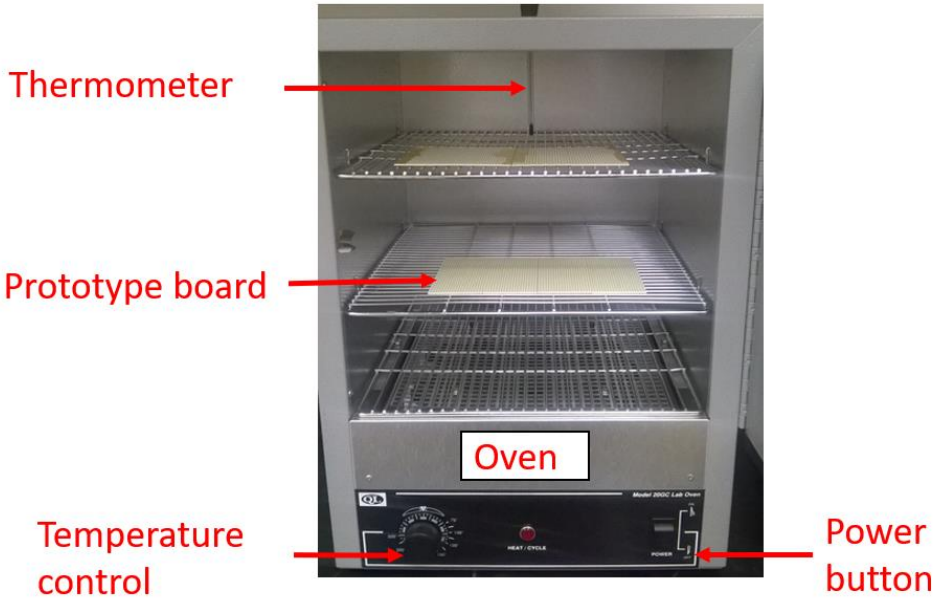

Figure 3. Curing Oven

Figure 4 presents the realized antenna layout, juxtaposed with a U.S. penny for scale. Once made, the piece was inspected for any flaws using a Keyence VHX-7000 advanced digital microscope. An enhanced image, showcasing the radiating patch and ground section's printed lengths, is featured in the red inset of Figure 4.

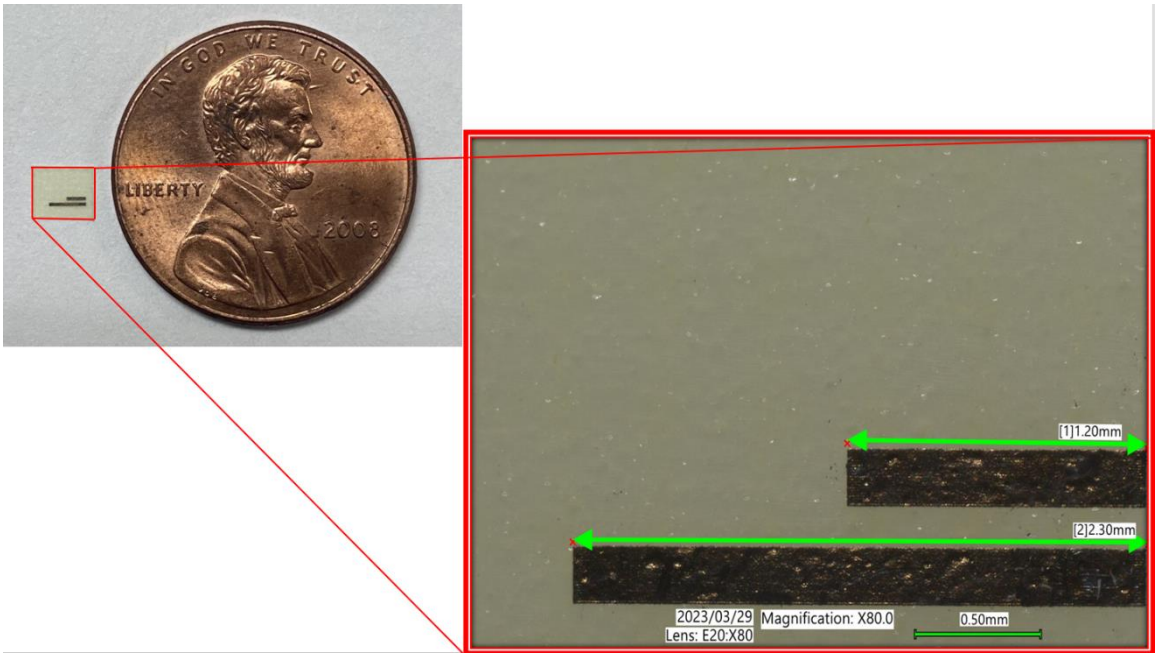

Figure 4. Fabricated antenna next to United States one-cent coin. Magnified image, obtained from high-resolution digital microscope, is shown in red insert.

3.6 Performance Testing and Results.

The simulated outcomes of the suggested antenna are shown, comparing return loss (S11), the polar representation of THz radiation, and a 2D directional radiation graph on the H-plane. A common hurdle for THz antennas is obtaining the required calibration tools and electronic parts for examination and measurement. Currently, the constructed antenna is under evaluation, with results up to the maximum THz frequency expected to be updated in this documentation soon.

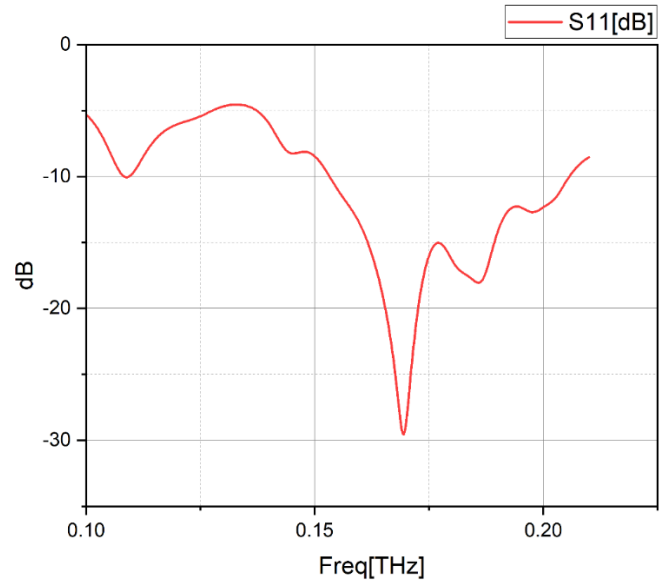

Figure 5. S11 Plot (0.1 – 0.21 THz)

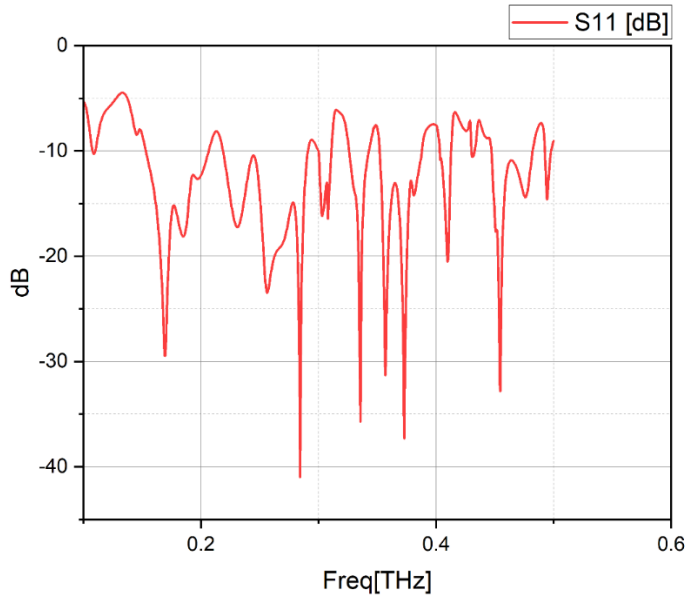

Figure 6. S11 Plot (0.1 – 0.45 THz)

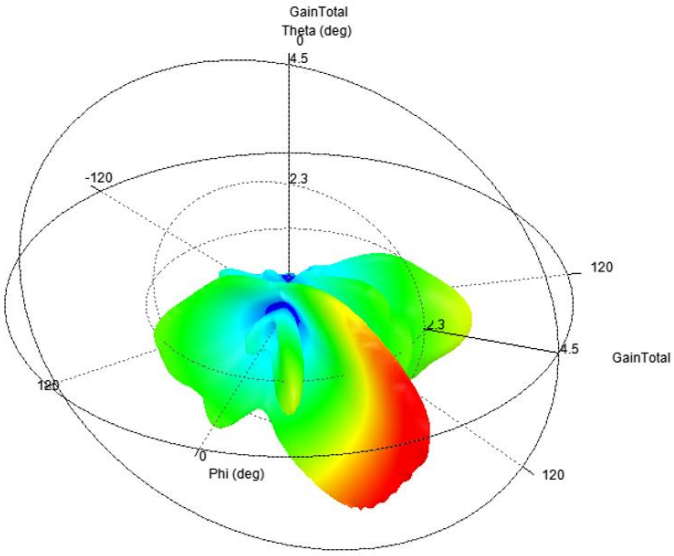

Figure 7. Polar Plot

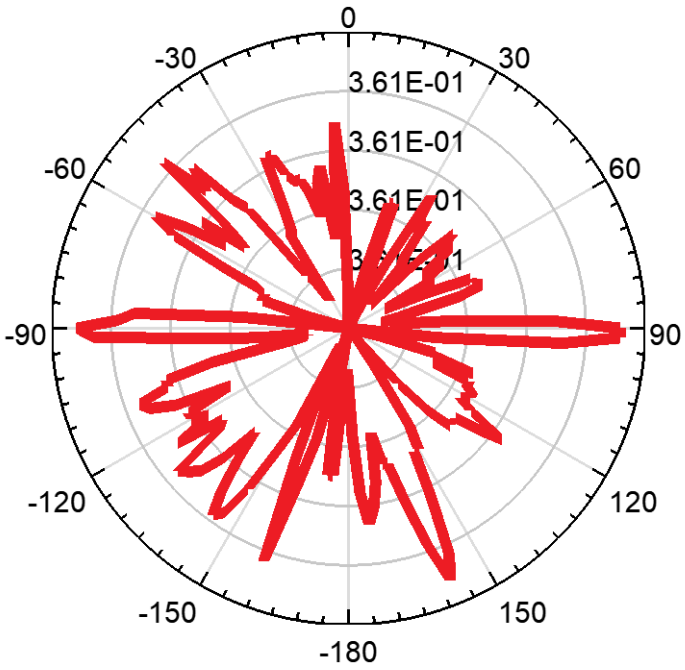

Figure 8. Radiation Pattern

Figures 5 and 6 present the S11 Plot data (ranging from 0.1THz – 0.21THz and 0.1THz – 0.45THz respectively), Figure 7 illustrates the polar graph, while Figure 8 highlights the radiation pattern from Ansys HFSS v2022 tool. Based on these simulations, the antenna exhibits a multi-directional radiation graph in the H-plane at 0.125 THz, having a top gain of 0.38dB. This quality can be beneficial in scenarios demanding widespread radiation patterns, such as indoor setups, close-distance communication tools, or sensing functions. The antenna's multi-directional quality is seen as beneficial for prospective Many-Input-Many-Output (MIMO) systems due to its direction selectivity. The antenna possesses impedance ranges at intervals of 0.1535THz-0.206THz, 0.2175THz-0.2903THz, 0.326THz-0.3427THz, and 0.352THz-0.388THz.

The terahertz antenna model displays promising simulation data, particularly multi-directional radiation designs on the H-plane at 0.125 THz with a top gain of 0.38dB. The antenna's ability to radiate in multiple directions holds potential for upcoming Many-Input-Many-Output (MIMO) systems, promoting improved direction focus and selection. The antenna also boasts broad impedance ranges, fitting numerous Terahertz communication setups. Nevertheless, the main obstacle is securing the necessary calibration tools and electronic parts for the Terahertz spectrum testing. The constructed antenna's examination is ongoing. The introduced Terahertz antenna layout, backed by the Ansys HFSS v2022 tool's simulations, underlines its capacity to push forward Terahertz communication studies, setting the stage for futuristic wireless systems and uses.

3.7 Comparison of THz Antenna with Traditional Designs.

In comparing THz antennas with traditional designs, a notable difference lies in scale and precision. THz antennas, such as design antenna in this study, are significantly smaller due to the shorter wavelengths at terahertz frequencies. This reduction necessitates meticulous fabrication techniques to ensure functionality at the intended frequency. Additionally, THz antennas often require advanced materials to mitigate losses and maintain signal integrity, where traditional designs might rely on more conventional materials and components.

Another critical aspect is the feeding mechanism, which, in THz designs, must be exceptionally precise to accommodate the compact structure and high frequencies. THz antennas also exhibit a higher sensitivity to manufacturing tolerances, which can substantially affect the S-parameters, indicative of the antenna's performance. From the plot results, the proposed THz antenna showcases how efficiently it transmits and receives electromagnetic waves, with minimal reflection and optimal impedance matching, which are pivotal for ensuring the high-resolution capabilities required in THz applications.

Finally, the simplicity of the design of the antenna distinguishes it from other THz antennas.

3.8 Challenges and Solutions.

The challenge encountered during the fabrication of the THz antenna was “spreading” after sintering. This was because of the nozzle size that was initially being used and caused an increase in dimension of the initial prints. To eliminate this, the nozzle size had to be reduced to 100um printer tip, which resulted in a well-defined print.

The designed and fabricated antenna is currently undergoing testing. The major challenge with the THz spectrum is limited resources for testing and verification. This is because it is still a newly explored spectrum. Due to this limitation, the antenna can only be tested between 10-110GHz.

3.9 Real-World Application Scenarios for the THz Antenna.

From the plot results, it is evident that the implementation of the proposed THz antenna design in real-world application scenarios is both promising and diverse. The capabilities of the THz antenna, as shown in the simulation results, suggest potential use in high-speed wireless communication networks, marking a significant stride towards next-generation connectivity. This could lead to revolutionary changes in fields such as telemedicine, where instantaneous data transfer is critical. Furthermore, given the high-frequency precision of the THz antenna, it could be instrumental in advanced sensing applications, such as detecting minute defects in industrial settings or facilitating secure communication channels in defense sectors. The simulated performance, particularly in terms of efficiency and bandwidth, implies that this antenna can be a keystone in devices

meant for immersive experiences like augmented and virtual reality. As the push for faster and more reliable data transmission intensifies, the real-world applications for the THz antenna, backed by these simulations, seem poised to address the pressing demands of our evolving digital ecosystem.

Chapter 4: Balun Design and Fabrication

4.1 Introduction to Baluns.

Transmission line theory delves into the intricacies of impedance matching and its associated assumptions. A notable case involves connecting a 50 Ω coaxial cable (unbalanced) to a 50 Ω twin lead transmission line (balanced). Even with matching impedances, mismatches can occur due to differences in electric and magnetic fields between these lines. This becomes evident when we understand that a coaxial cable has an unbalanced electromagnetic mode, while a twin lead transmission line possesses a balanced mode. Though they might have the same characteristic impedance, their electromagnetic fields are distinct. This mismatch arises not just from impedance differences but from the distinct fields and modes of transmission lines. Distributed circuit analysis, as described by Chipman, is grounded on several postulates, including the uniformity of transmission lines and specific behavior of currents and potentials. However, when connecting two different transmission lines, such as a coaxial and a twin lead with identical impedances, these postulates can be violated. As such, a mode transformer or balun becomes essential to ensure effective signal transition between unbalanced and balanced lines, especially in antenna engineering scenarios where unbalanced feeds are often required.

In the realm of antenna systems, baluns play a crucial role in transitioning between balanced antenna structures and unbalanced transmission lines. Passive baluns constructed using transformers, transmission lines, or discrete components, operate without external power. Their inherent simplicity and reliability make them a staple in

many traditional antenna setups, although they can introduce some losses, particularly at elevated frequencies. In contrast, active baluns, incorporating components like amplifiers, require external power sources. While they offer the potential to boost signals, an attribute beneficial for compensating for antenna system losses or supporting longer transmission paths, their complexity might lead to additional noise or signal distortion. The selection between these two balun categories is guided by the specific antenna application, operational frequency, and desired signal fidelity.

4.2 Balun Design Principles for Targeted Frequencies.

Baluns come in many shapes and sizes, each made for different types of radio frequencies. Coaxial baluns are good because they can block out background noise, which makes them popular for radio frequency (RF) use. Ferrite core baluns are also good for high-frequency signals because they can match different impedances and cut down on noise.

In electronics that use integrated circuits, microstrip and strip-line baluns are key. They're built right onto circuit boards and take advantage of the board's own ability to carry signals. They're small and flexible, which is great for RF and microwave tech that needs to fit into tight spaces.

Transformer baluns work by wrapping wire around a core to change impedance levels. They can work with a range of frequencies, which makes them very versatile. Tapered

baluns gradually change impedance, which is good for equipment that needs to work well over a wide range of frequencies.

When choosing a balun, you must think about the frequency it'll work with, the bandwidth you need, and what the balun needs to do in your specific project to make sure it sends signals well.

Creating a balun that operates efficiently over a desired frequency range requires a mix of engineering principles and precise calculations. The necessary considerations and calculations required in designing a balun are listed below:

1. Turns Ratio for Impedance Matching:

The ratio of turns in the balun's windings is determined by the square root of the output to input impedance ratio:

Turns Ratio (N): $N = \sqrt{\frac{Z_{out}}{Z_{in}}}$

2. Symmetry for Balanced Operation:

Ensuring symmetry in the design is crucial, though this is more about the physical layout than a specific calculation.

3. Frequency Bandwidth Relationship:

The bandwidth, related to the quality factor and central frequency, is given by:

$$\text{Bandwidth (BW)} = \frac{\text{Central Frequency } (f_c)}{\text{Quality Factor (Q)}}$$

The quality factor itself depends on the inductance and resistance at the operating frequency:

$$\text{Q} = \frac{\text{Inductive Reactance } (X_L)}{\text{Resistance (R)}}$$

4. Quarter-Wavelength Transformer Principle:

For certain balun types, the length of the line is a quarter of the wavelength at the design frequency:

$$\text{Line Length } (\ell) = \frac{\text{Phase Velocity } (v_p)}{4 \text{ x Central Frequency } (f_c)}$$

5. Effect of Material Properties:

The dielectric properties of the substrate influence the wavelength and must be factored in:

$$\text{Wavelength } (\lambda) = \frac{\text{Speed of Light (c)}}{[\sqrt{\text{Effective Dielectric Constant (eff)}}] \text{ x Frequency (f)}}$$

6. Calculation of Inductance and Capacitance:

The inductance and capacitance values are determined by the physical dimensions and properties of the materials:

$$\text{Inductance (L)} = \frac{\text{Permeability } (\mu) \text{ x Turns2 x Area (A)}}{\text{Length } (\ell)}$$

$$\text{Capacitance (C)} = \frac{\text{Dielectric Constant } (\varepsilon) \text{ x Area (A)}}{\text{Distance (d)}}$$

7. Assessing Reflection and Return Loss:

The reflection coefficient and return loss tell us how much signal is reflected due to an impedance mismatch:

$$\text{Reflection Coefficient } (\gamma) = \frac{\text{Load Impedance } (Z_{load}) - \text{Characteristic Impedance } (Z_0)}{\text{Load Impedance } (Z_{load}) + \text{Characteristic Impedance } (Z_0)}$$

$$\text{Return Loss (S11)} = -20 \times \log_{10} (|\gamma|)$$

In our study, we made a microstrip/strip-line balun that works at microwave frequencies (1GHz to 300GHz). Our 40x40mm balun is nice and small, which is important in small gadgets. It's not just compact; it also fits well with other electronics. The strip-line part also blocks outside noise, making sure the balun works the way we expect. This design is a good middle ground: it's affordable, not too tricky to make, and it performs well. With so many kinds of baluns out there, our 40x40mm microstrip/strip-line balun stands out as a smart and effective option for today's communication technology.

4.3 Design, Simulation, and Prototyping of Baluns.

Design Considerations:

Balanced Design: The layout is symmetrical, which is essential for ensuring uniform outputs in balun configurations. Such balance contributes to dependable performance.

Space-Saving Layout: The size of the balun (40x40 mm), ensures that it is streamlined, making it advantageous for incorporation into systems with spatial constraints.

Clear Traces: The conductive routes, or traces, are distinctly outlined. This clarity is pivotal for efficient signal transfer and reducing undesirable side effects.

Material Choice: The selected substrate materials, flexible and rigid FR4 substrate, profoundly influences the balun's functionality. This is because it is vital that the substrate ensures excellent insulation and possesses the right dielectric qualities for its target frequency range.

Component Compatibility: The balun is designed in such a way that makes it adaptability with other components or setups when paired with other models or systems.

Manufacturing Considerations: The balun design is unambiguous. Yet, the exactness needed in crafting those routes and material selection remains paramount.

The microstrip balun has a square form and measures 40 mm in length. The unbalanced input line is 1.2 mm wide, while the two balanced output lines are each 0.7 mm wide. The space between these ports is 0.6 mm. Every port, both balanced and unbalanced, is set to 50 Ohms for easy measurement. These lines have assigned lumped ports and are assigned excitation. We also made a radiation enclosure, double the balun's size, with a specific radiation boundary.

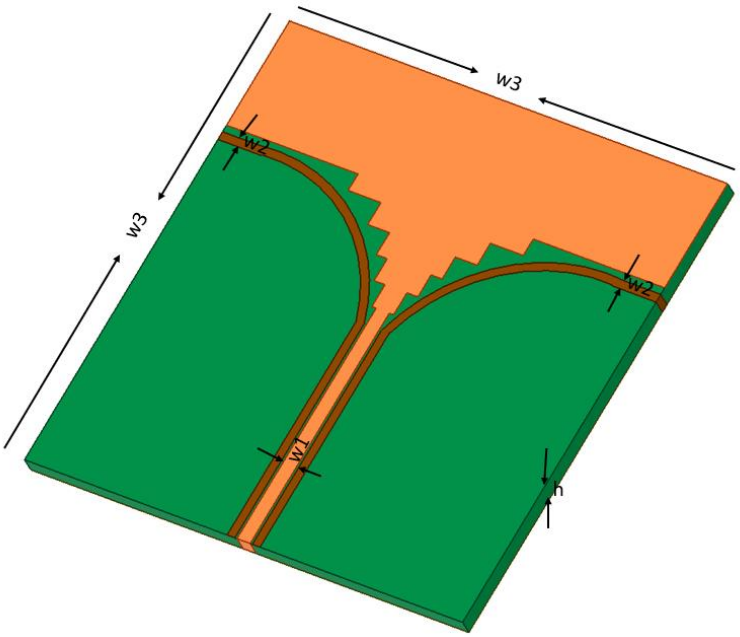

Figure 9. Ansys HFSS simulation balun dimensions: w1 = 1.2 mm, w2 = 0.7 mm, w3 = 40 mm, h = 1.5 mm (0.16mm for flexible substrate).

We carried out simulations based on real-world production standards, both for a solid FR4 substrate and a flexible one. The solid FR4 material was given a thickness of 1.5 mm with a dielectric constant (εr) of 4.4. The flexible FR4 simulated substrate was made 0.16 mm thick with a dielectric constant (εr) of 3.4. The substrate sits on a ground plane with a perfect electric (Perfect E) boundary. The radiating coupled microstrip lines are positioned on the FR4 substrate and have a perfect electric (Perfect E) boundary. The performance of the balun is done at a 2 GHz frequency, scanning at adjusted frequencies

in a linear fashion, ranging from 1 GHz to 25 GHz. We then generated plot reports to investigate specific data related to the S parameter's phase and strength in the XY terminal.

MANUFACTURING METHODS

A. PCB:

The blueprint was taken from the Ansys simulation program as a DXF file and inputted into KiCad to yield the gerber file format essential for PCB development. These files were then delivered to Sunstone Circuits Company for development. FR4 rigid substrate was chosen, and the design's coupled strip lines were crafted using copper.

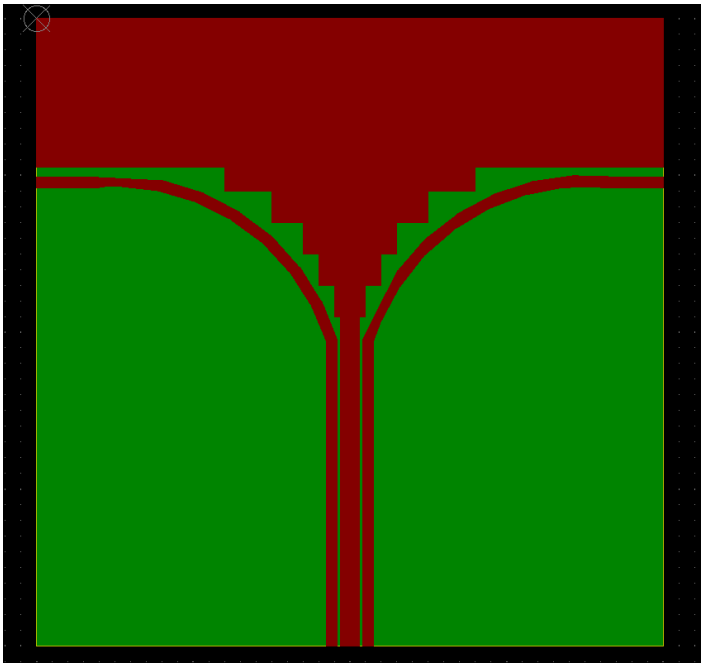

Figure 10. *Extracted Gerber File, from KiCad.*

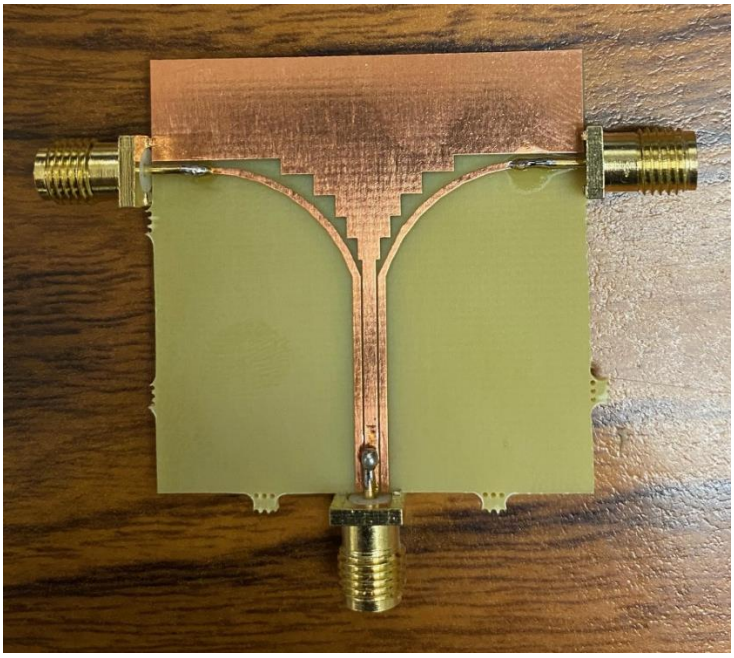

Figure 11. Fabricated PCB design with soldered SMA connectors.

B. Screen-Printing:

The exported balun design from Ansys HFSS was converted into CAD format. A stainless-steel screen mesh stencil was produced, having a thickness that matched the LF-350 Copper paste's viscous consistency and the aimed print trace thickness.

The copper paste (manufactured and supplied by Copprint Technologies Ltd), once conditioned to room temperature from cold storage, was briskly stirred to distribute copper granules evenly and prevent settling.

The dielectric, a flexible FR4 material fit for RF uses, was chosen for its dielectric constant and loss tangent characteristics. The substrate was cleaned, removing dust and possible pollutants.

During the printing process, the substrate was stabilized on a working platform, with the screen mesh positioned above. Proper alignment of the design with the base was ensured.

To achieve a tilt in the screen mesh, a 3mm thick book was employed. The paste was then laid on the mesh, and a polyurethane squeegee was used to disperse it. The squeegee ensured the paste passed through the mesh's design openings onto the substrate. Uniform paste application was ensured through consistent squeegee speed and angle.

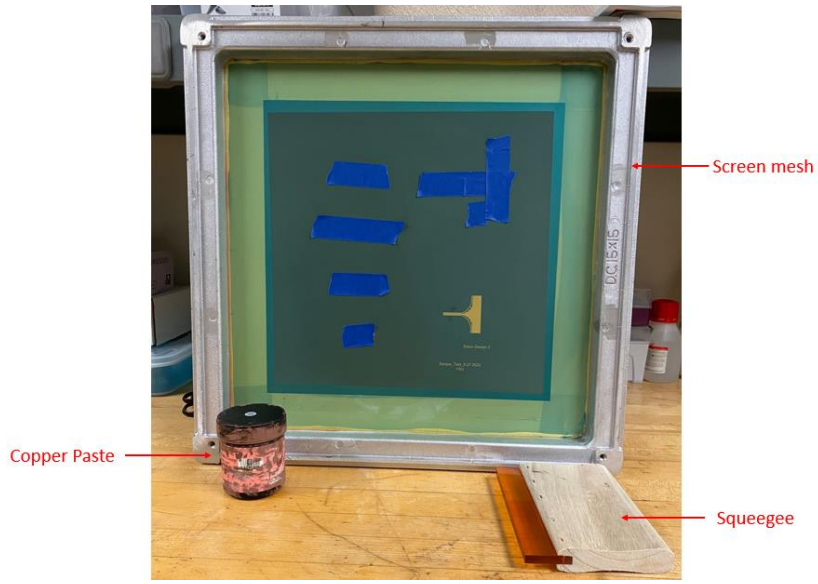

Figure 12. Screen Mesh, Squeegee and LF-350 Copper paste from Copprint.

A two-phase curing process followed: an initial 80°C drying on a thermal plate for solvent evaporation, followed by a 450°C lamination process, with the printed design wrapped in baking paper, to sinter the copper granules into a cohesive, conductive trace.

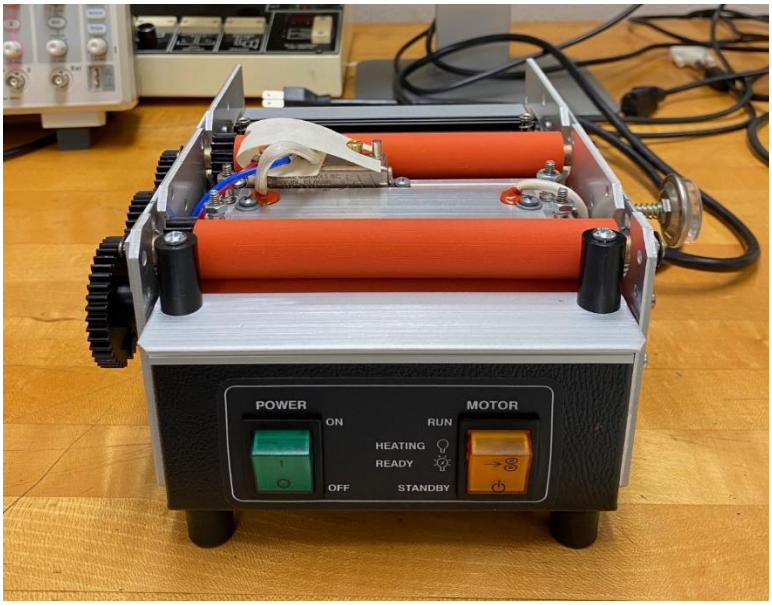

Figure 13. Laminator used in curing process.

Optical microscopy was then used to assess trace quality, followed by a conductivity test using a multimeter to detect any flaws.

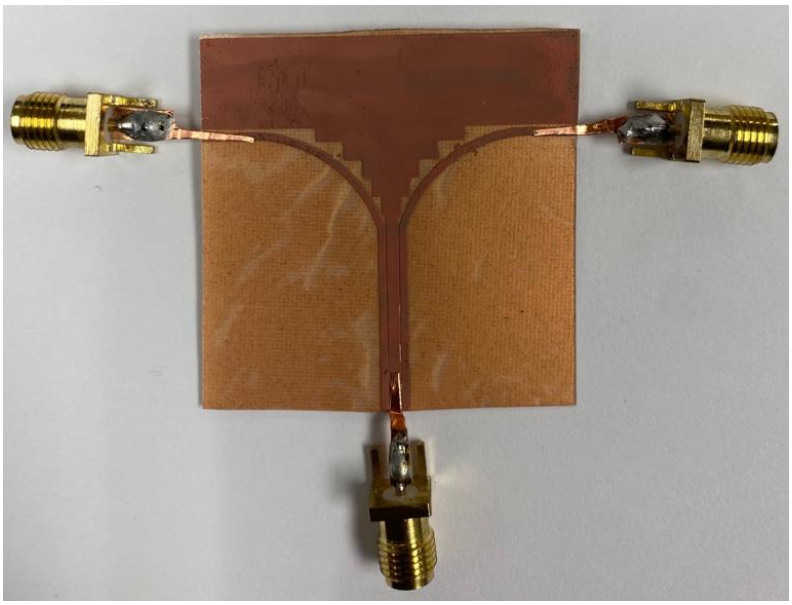

Figure 14. Screen-printed Balun on flexible FR4 after curing.

C. Aerosol Jet Printing (via IDS):

The balun blueprint was sourced from Ansys HFSS as a DXF file, then modified in Fusion 360 to adjust scale, set the optimal print orientation, and process the slicing parameters. The resulting file was then imported into the IDS printer.

Once again, a cleaned flexible FR4 substrate was chosen based on its specific electrical properties.

Silver nanoparticle ink, combined with terpineol, was deposited in the IDS machine's ink cartridge, which was then linked to the device's atomizer base and flow cell. Machine parameters were optimized using Flow Vision and FlashCut CNC. These settings managed gas flow, voltage, temperature, print specs, jetting rate, and movement speed to guarantee precise deposition and resolution. In the machine, the atomizer transformed the ink into an aerosol, transported to the print nozzle by nitrogen gas, and then meticulously sprayed onto the flexible substrate. This layering continued until the balun reached the desired thickness.

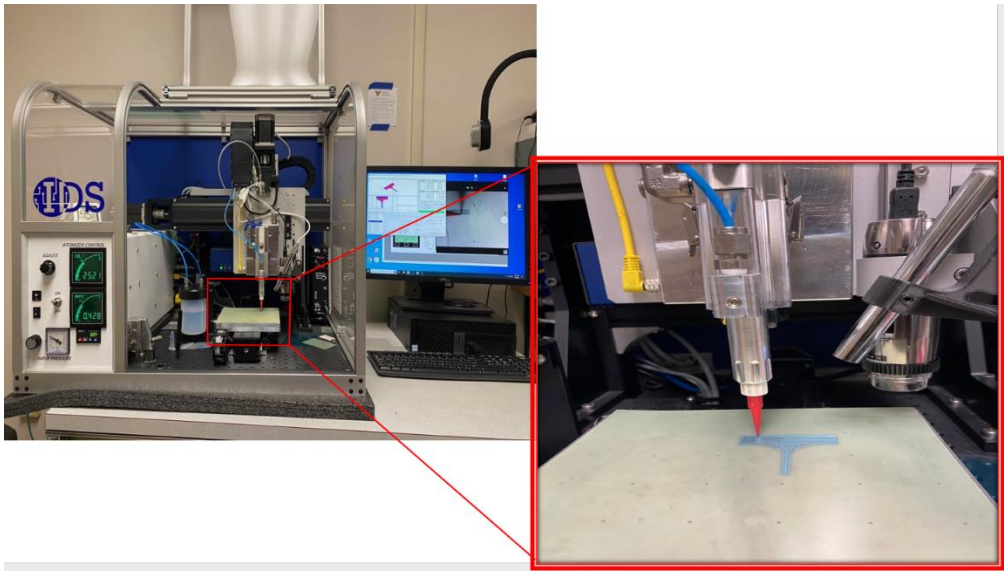

Figure 15. IDS machine with highlighted print of Balun design.

Post-printing, the design underwent a two-tiered curing process in a vacuum chamber: 30 minutes at 80°C for solvent evaporation and another 30 minutes at 250°C for sintering, ensuring a smooth transition of nanoparticles into connected conductive routes.

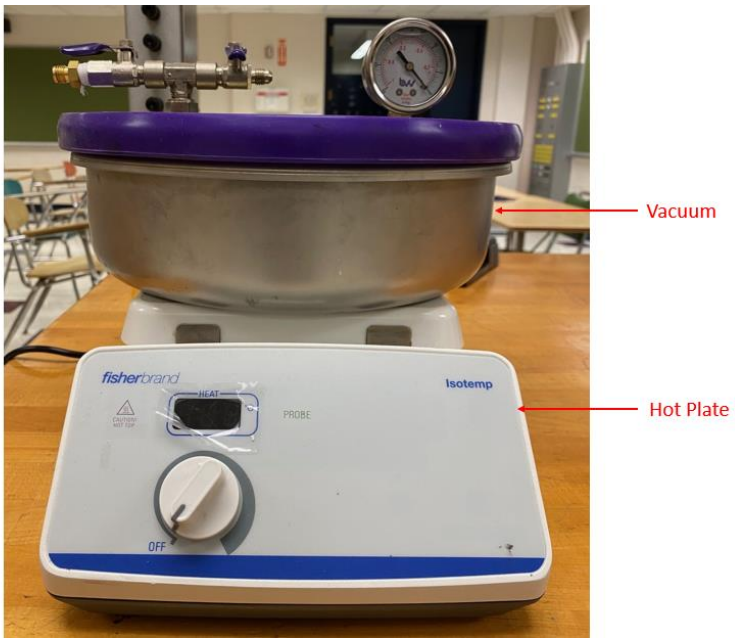

Figure 16. Vacuum and Hot plate used for curing.

A high-magnification microscope inspected the final design, followed by a multimeter-conducted conductivity check.

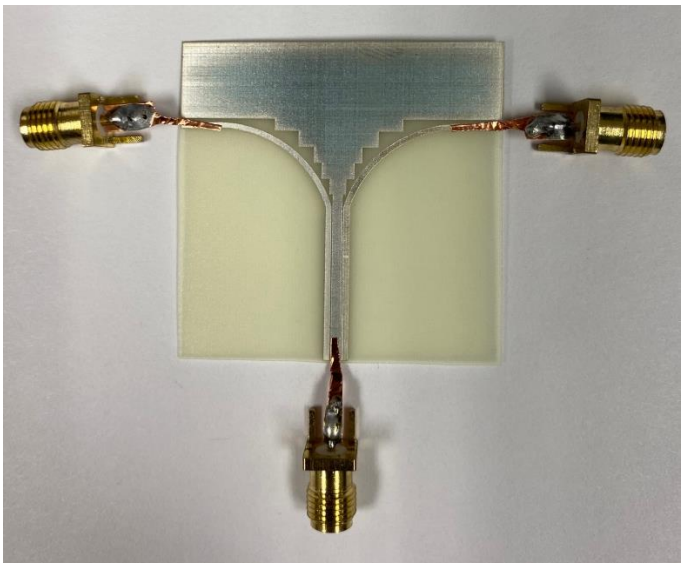

Figure 17. AJP Balun design after curing process.

4.4 Performance Analysis and Results.

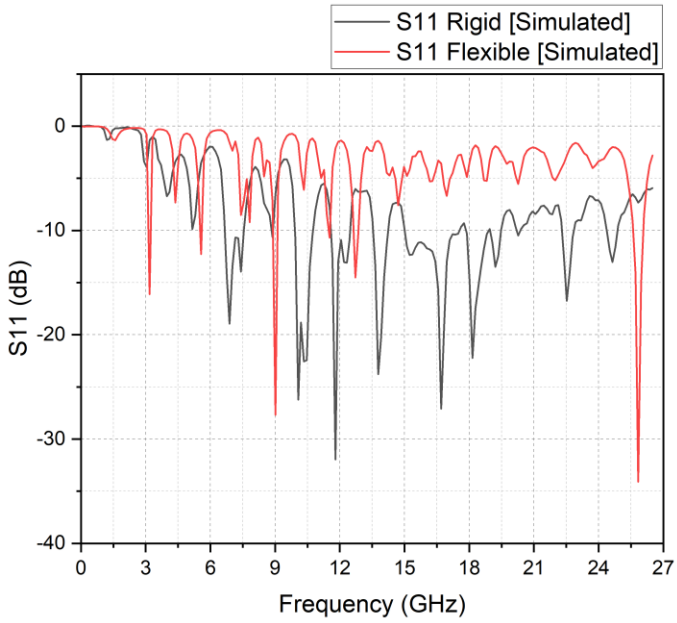

Figure 18. Simulated S11 parameter plot [Rigid vs Flexible]

Fig. 18 displays the comparative S parameter simulations for both solid and flexible materials, using the Ansys Electronics 2022 R2 software.

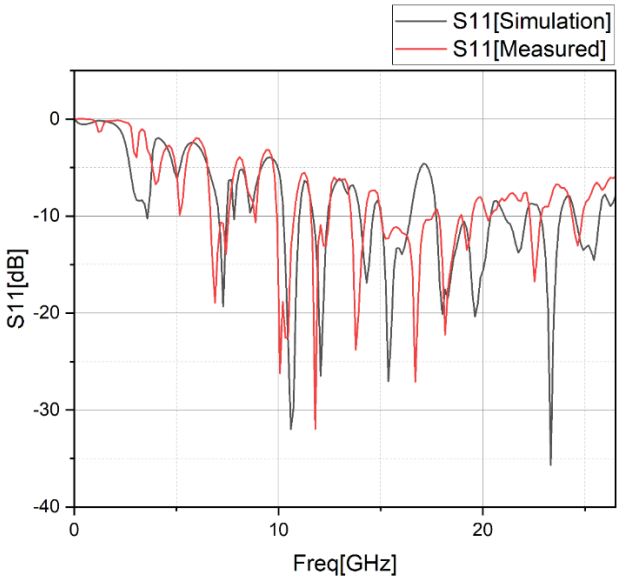

Figure 19. Rigid substrate S11 parameter plot [Simulation vs Measured]

Fig. 19 compares S parameter simulations for the rigid material from the same software against data from the Keysight ENA Network Analyzer E5080. Notably, the return loss was consistently better than -10 dB between 10.11 GHz and 10.85 GHz in both simulated and real measurements.

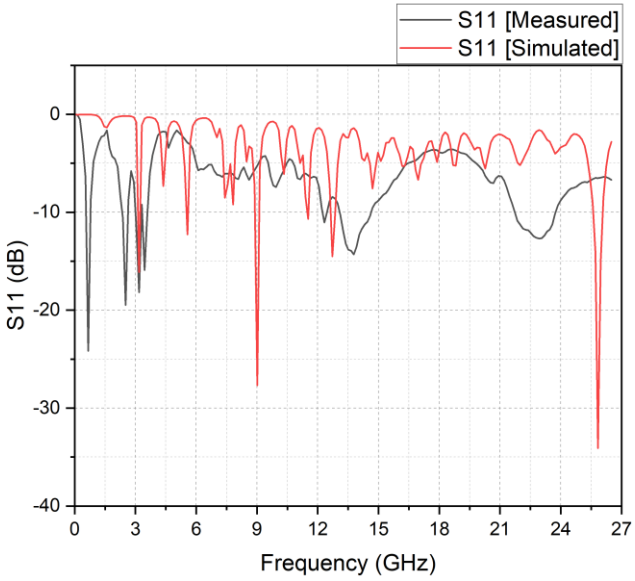

Figure 20. Screen-printed S11 parameter plot [Simulation vs Measured]

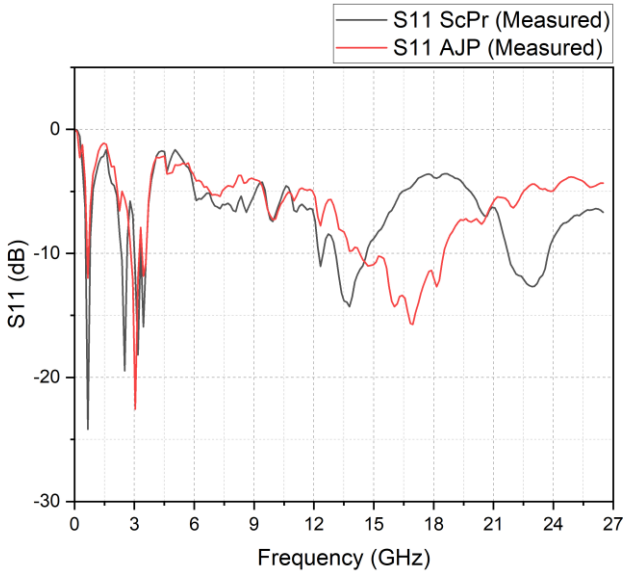

Figure 21. Flexible Substrate S11 parameter plot [AJP vs Screen-printed]

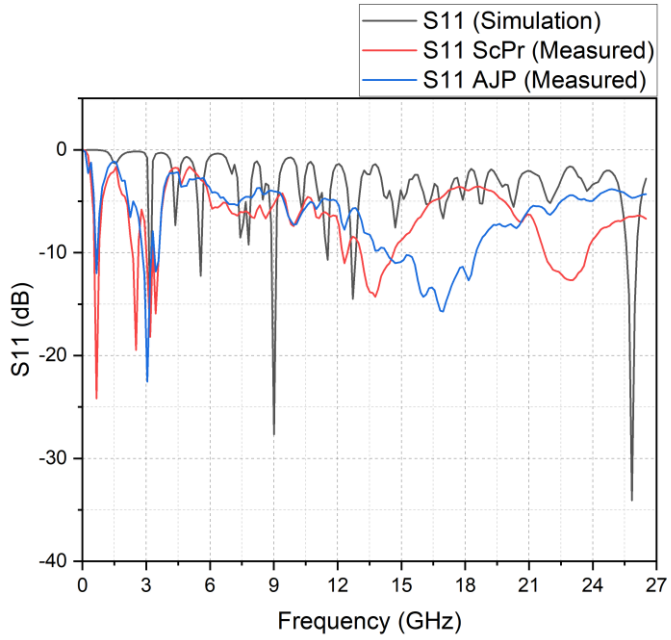

Figure 22. Flexible Substrate S11 parameter plot [Simulation vs Screen-printed vs AJP].

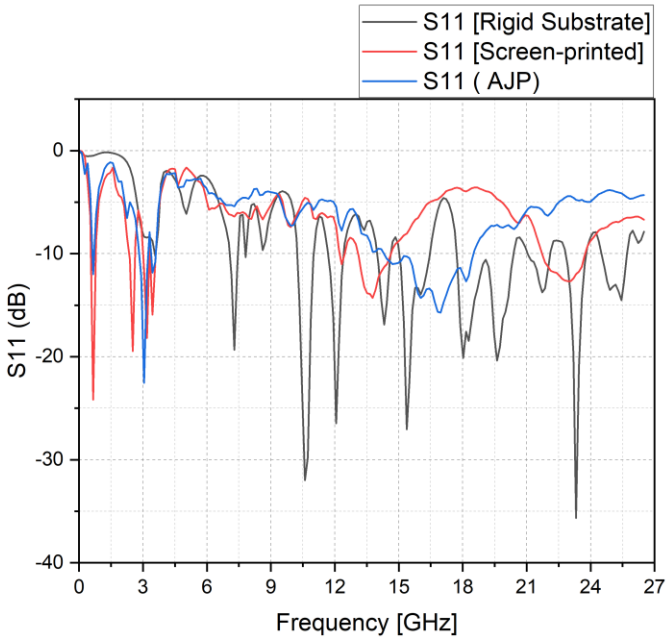

Figure 23. Measured S11 Plot of PCB vs Screen-Printed vs AJP.

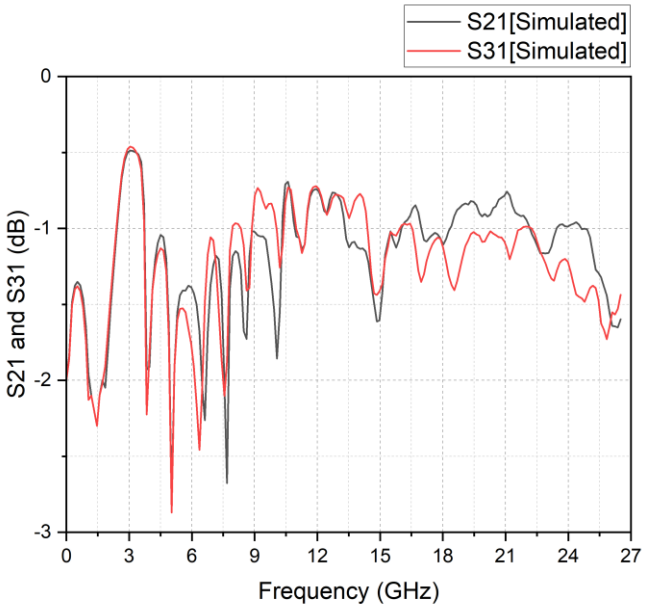

Figure 24. Rigid substrate S21 and S31 parameter plot [Simulation]

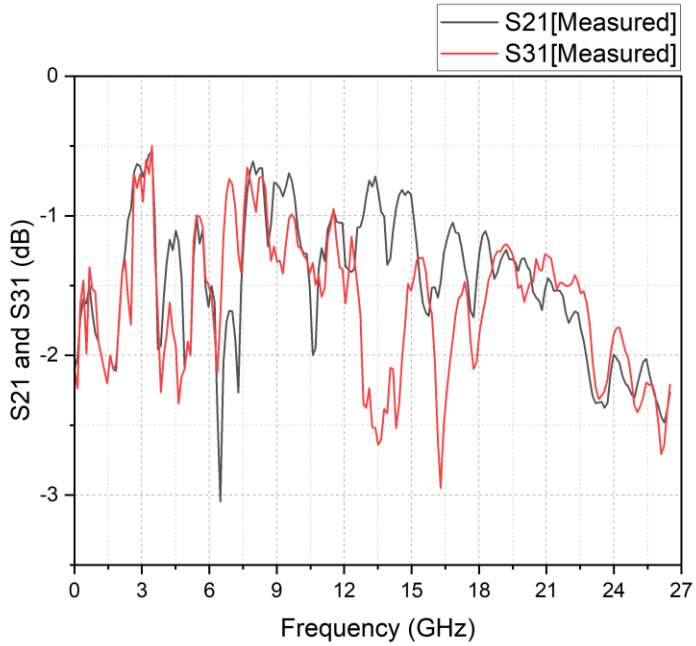

Figure 25. Rigid substrate S21 and S31 parameter plot [Measured]

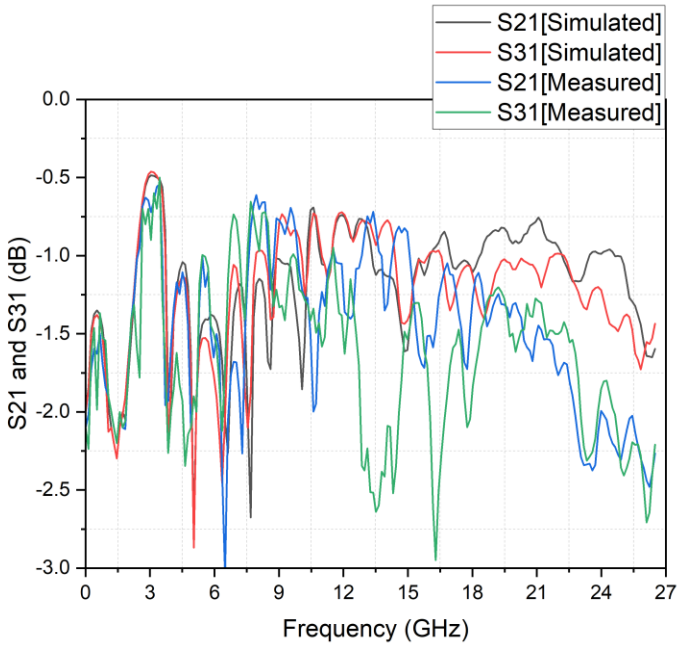

Figure 26. Rigid substrate S21 and S31 parameter plot [Simulation vs Measured]

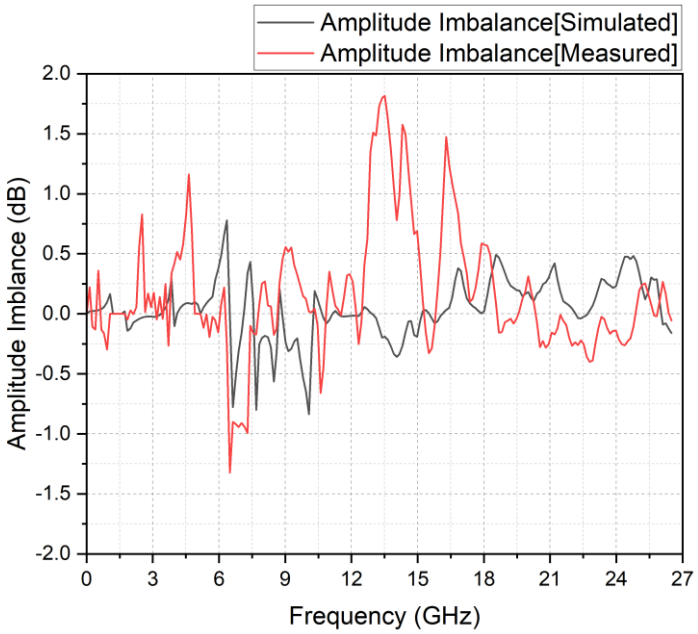

Figure 27. Rigid Substrate Amplitude Imbalance [Simulation vs Measured]

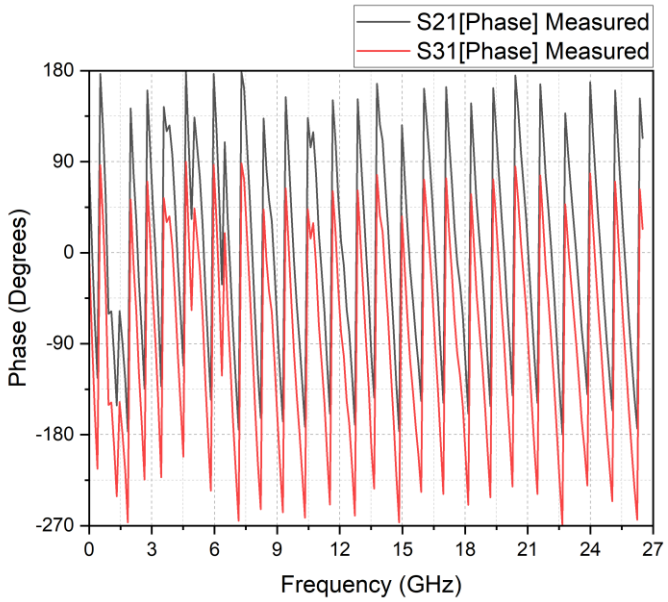

Figure 28. Rigid Substrate Phase Response

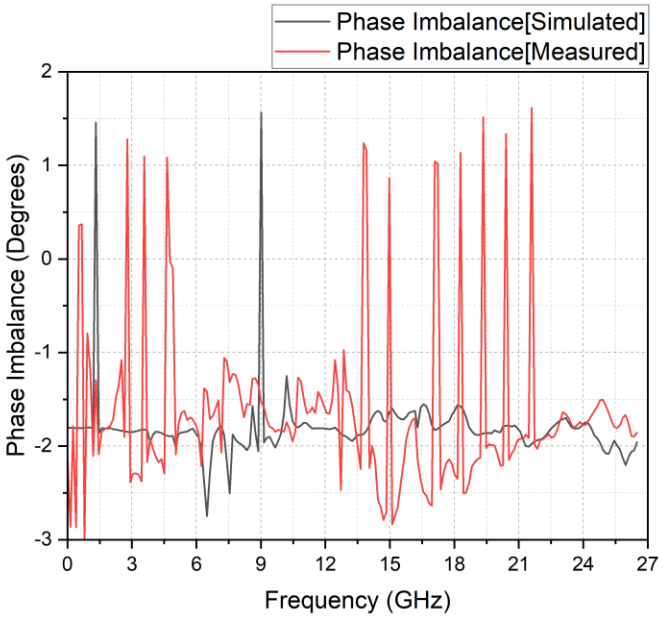

Figure 29. Rigid Substrate Phase Imbalance

Fig. 27, 28, and 29 depict differences in amplitude, phase response, and phase imbalance between the measured and simulated results, represented by |S21|-|S31| and <S21-<S31

minus 180 degrees. Fig. 4 provides a visual of the finished balun design. When evaluating the designs made by three different manufacturing techniques, certain features stood out. Both the PCB and AJP methods, which relied on advanced lithographic processes, displayed finer detail. The AJP achieved this due to its specific nozzle size, whereas screen-printing was more restricted by the mesh size. This resulted in larger designs compared to PCB and AJP. The PCB and AJP methods produced smoother finishes, while screen-printing was somewhat coarse, affected by paste consistency. The PCB process yielded uniform thickness thanks to its precise etching and deposition, much like the AJP's uniform layering, which was influenced by optimized settings. Screen-printing, however, depended on the mesh and application pressure, leading to potential thickness variations. Examining RF and electric performance metrics from the VNA device revealed specific traits depending on the material used. For the solid FR4 material, there were two significant bandwidths with return losses under -10 dB. One spanned from 3.1285 GHz to 3.2317 GHz, and the other from 8.8960 GHz to 9.1143 GHz. This suggests the balun can function in two separate frequency bands on solid materials. However, on flexible materials, the balun worked well across different bands, notably from 7.06 GHz to 7.45 GHz, and then from 10.22 GHz to 10.99 GHz. The AJP-made design had a range between 2.92 GHz – 3.59 GHz and 14.3 GHz – 18.6 GHz. The performance variation between solid and flexible materials can be linked to factors like material properties, dielectric values, thickness, and flexibility, which affect the RF device's electromagnetic activity.

Therefore, the substrate's selection is crucial in balun design, as highlighted by the distinct bandwidths on different FR4 materials. By recognizing these material-specific

behaviors, RF specialists can better tailor their creations for particular uses and frequency bands.

4.5 Impact of Substrate Type (Rigid vs Flexible Substrate).

The measured S11 parameter graphs provide insight into the performance of the balun on two different substrates: a rigid and a flexible FR4 material. The S11 parameter, representing how much power is reflected from the antenna, indicates better performance with less reflection as the value approaches zero. From the plots, we can discern that the balun designed on a rigid FR4 substrate generally exhibits a lower reflection coefficient across the frequency spectrum, suggesting that it is better matched and hence, more power from the source is delivered to the antenna rather than being reflected. The flexible substrate, while showing a higher degree of reflection (higher S11 values), still achieves satisfactory matching at certain frequencies, indicating specific windows where it operates effectively. The flexible substrate introduces more variability in the performance, which could be due to its mechanical properties affecting the electrical characteristics. This variability is critical in applications where consistent performance is required across a broad frequency range. Overall, the choice of substrate can have a significant impact on the balun's performance, with rigid substrates offering more stability and potentially better overall performance than their flexible counterparts.

4.6 Use Cases for the Designed Balun in Communication Systems.

The measured S11 parameter plots for both flexible and rigid FR4 substrates offer insight into how the designed balun might perform in various communication system scenarios.

1. High-Frequency Communication Systems:

The balun's performance across a broad frequency range up to 20 GHz suggests its applicability in high-frequency systems, such as satellite communication, where high bandwidth and efficient signal transmission are critical.

2. Flexible Electronics:

The flexible substrate's S11 performance indicates that this balun can be suited for emerging flexible electronics, which could include wearable devices, flexible smartphones, or other adaptive communication systems.

3. Wireless Networking:

The resonant points in S11 plots, indicating better matching at specific frequencies, could be exploited in wireless networking for specific bands, enhancing signal integrity and reducing reflection losses in systems like Wi-Fi, 5G, and potentially 6G technologies.

4. Test and Measurement Equipment:

The precise and stable performance at certain frequencies makes the balun suitable for test and measurement equipment, where accurate signal characterization is paramount.

5. Military and Aerospace:

Given the rigid substrate's stable performance at lower frequencies and high durability, such baluns could be utilized in military and aerospace applications where robustness is essential.

6. Phased Array Radar Systems:

Phased array systems, which require precise phase and amplitude control, could benefit from the consistency shown in the S11 parameters over the given frequency range.

Each use case would require the balun to maintain performance characteristics in line with the observed S11 parameters, ensuring low reflection coefficients at the desired operating frequencies for optimal functionality.

Chapter 5: Conclusions and Future Work

5.1 Summary of Key Findings.

The research conducted on THz antenna and balun design culminates with significant findings for THz communications and RF engineering. The novel THz antenna design demonstrates a multi-directional radiation pattern, advantageous for MIMO systems, with a peak gain of 0.38dB at 0.125 THz and substantial impedance bandwidths across four distinct THz frequency ranges. The comprehensive study on balun fabrication reveals that PCB and AJP methods yield superior resolution and smoother finishes, while screen-printing results in coarser features due to limitations in paste viscosity control. Moreover, the performance analysis on various substrates underscores the criticality of substrate choice in balun design, with the rigid FR4 substrate exhibiting dual-band operation and the flexible substrate showing versatility across different frequency bands. These key findings underscore the influence of substrate material and fabrication techniques on the performance of RF devices and provide a foundation for tailored design strategies in advanced THz communication systems.

5.2 Contributions to the Field.

This thesis contributes to the field of terahertz (THz) communications by presenting an innovative THz antenna design and a dual-band balun for impedance matching and transition efficiency. Our work bridges the gap between theoretical design and practical application by advancing the efficiency and performance of THz antennas. By

meticulously calculating the antenna dimensions to resonate precisely within the THz spectrum, the design ensures optimal wavelength utilization and signal strength. The dual-band balun, a novel addition, effectively addresses impedance mismatches, significantly enhancing the overall performance of any system it is implemented. The fabrication techniques used for both the THz antenna and the balun show how the cost of production and reduction of waste can be achieved, while still getting optimal performance from the components. We also see how the choice of substrate is critical in the performance of a balun. This contribution not only demonstrates the feasibility of more compact and efficient THz antennas and baluns but also sets a new benchmark for future research and development in ultra-high-speed wireless communication systems.

5.3 Implications for Future Communication Infrastructure.

The growth and use of THz antennas, along with new methods in printed balun production, mark significant changes in our communication systems. The THz frequency range offers extremely fast data transfer speeds, making it a key area for future wireless tech. Reliable components like antennas and baluns become more and more vital as we dive deeper into this range. Using modern tools like Ansys HFSS and fabrication methods like Aerosol Jet Printing ensures these parts work well in the THz range. Printed baluns on RF-optimized materials, such as FR4, point to a future with more flexible communication gear. This adaptability might lead to smaller, but powerful communication tools, perfect for new tech like wearables and IoT devices. As 6G

technology starts to emerge, THz antennas and printed baluns will play a big role in creating a faster, more connected world.

5.4 Societal and Industrial Impact.

The rise of THz antennas and the improvements in printed baluns are setting the stage for big changes in both society and industry. For everyday people, using THz frequencies means faster and better wireless communication, meeting the growing need for quick data. This speed could change the way we use augmented reality, virtual meetings, and online media. In healthcare, faster data could lead to better remote care and quicker treatments. For businesses, the strength and flexibility of printed baluns enhance the power of THz antennas, allowing for stable communication networks. This is crucial in fields like manufacturing, shipping, and transport where real-time data is key. The efficient production of printed baluns also means cost-saving and scalable communication tools, opening doors for many industries. Overall, the blend of THz antennas and printed baluns could lead to new advancements, making tech more efficient and widely available.

5.5 Critical Insights and Innovations.

The realm of THz antennas and baluns has witnessed remarkable advancements, with these innovations promising to revolutionize communication systems. THz antennas, operating in a previously unexplored frequency range, possess the potential for ultra-high-speed data transmission, marking a significant leap from existing communication

standards. The introduction of baluns, especially when fabricated using cutting-edge techniques, ensures that these antennas can function optimally. Innovations in tools, like the Ansys HFSS simulation software, have been pivotal in refining the design and performance of these components. Moreover, the flexibility of printed baluns on substrates like FR4 highlights the adaptability of these components, opening avenues for diverse applications beyond traditional communication systems.

5.6 Recommendations.

Given the groundbreaking nature of THz antennas and baluns, there are a few recommendations for stakeholders in this domain. Firstly, continuous investment in R&D is vital to further optimize the performance of these antennas, especially as we delve deeper into higher frequency ranges. Collaboration between academia and industry can accelerate the pace of these innovations. Secondly, training programs should be initiated for professionals to familiarize them with the nuances of THz technology, ensuring they are equipped to harness its potential. Finally, as technology keeps changing and improving, it's important to focus on setting standards. Creating steady and clear rules and ways of doing things will help make sure that as these parts become more common, they will work well with both current and upcoming communication systems.

5.7 Potential Future Research Directions.

Incorporation of photonic crystals into the THz design to improve the radiation efficiency, confine the THz wave within certain desired areas, reduce interference from surface waves and can be used to modify the refractive index around the antenna to change the characteristics of the resonance to any desired or targeted one.

We aim to develop a balun design focused on Terahertz (THz) frequencies, necessitating adjustments in the design's dimensions to fit the desired frequency band. Given the challenges in fabricating devices for terahertz frequencies using PCB techniques, our exploration will be confined to AJP methods for creating a design apt for terahertz usage. A balun crafted through AJP presents benefits like a reduced footprint, streamlined production, an expanded impedance range, and superior performance.

References

[1] K. B. Cooper et al., ‘‘A high-resolution imaging radar at 580 GHz,’ IEEE Microw. Wireless Compon. Lett., vol. 18, no. 1, pp. 64–66, Jan. 2008.

[2] K. Ahi, ‘‘Mathematical modeling of THz point spread function and simulation of THz imaging systems,’’ IEEE Trans. THz Sci. Technol., vol. 7, no. 6, pp. 747–754, Nov. 2017.

[3] S. Sung et al., ‘‘THz imaging system for in vivo human cornea,’’ IEEE Trans. THz Sci. Technol., vol. 8, no. 1, pp. 27–37, Jan. 2018.

[4] F. C. D. Lucia, D. T. Petkie, and H. O. Everitt, ‘A double resonance approach to submillimeter/terahertz remote sensing at atmospheric pressure,’ IEEE J. Quantum Electron., vol. 45, no. 2, pp. 163–170, Feb. 2009.

[5] R. Dickie, R. Cahill, V. Fusco, H. S. Gamble, and N. Mitchell, ‘‘THzfrequency selective surface filters for earth observation remote sensing instruments,’’ IEEE Trans. THz Sci. Technol., vol. 1, no. 2, pp. 450–461, Nov. 2011.

[6] R. Knipper et al., ‘‘THz absorption in fabric and its impact on body scanning for security application,’’ IEEE Trans. THz Sci. Technol., vol. 5, no. 6, pp. 999–1004, Nov. 2015.

[7] R. Appleby and H. B. Wallace, ‘‘Standoff detection of weapons and contraband in the 100 GHz to 1 THz region,’’ IEEE Trans. Antennas Propag., vol. 55, no. 11, pp. 2944–2956, Nov. 2007.

[8] X. Yu et al., ‘‘Exploring THz band for high-speed wireless communications,’ in Proc. 41st Int. Conf. Infr., Millim. Terahertz Waves (IRMMWTHz), Copenhagen, Denmark, Sep. 2016, pp. 1–2.

[9] E. Lacombe et al., ‘‘10-Gb/s indoor THz communications using industrial Si photonics technology,’ IEEE Microw. Wireless Compon. Lett., vol. 28, no. 4, pp. 362–364, Apr. 2018.

[10] S. Jia et al., ‘‘A unified system with integrated generation of high-speed communication and high-resolution sensing signals based on THz photonics,’ J. Lightw. Technol., vol. 36, no. 19, pp. 4549–4556, Oct.1, 2018.

[11] Z. Wu, M. Liang, W.-R. Ng, M. Gehm, and H. Xin, ‘‘Terahertz horn antenna based on hollow-core electromagnetic crystal (EMXT) structure,’’ IEEE Trans. Antennas Propag., vol. 60, no. 12, pp. 5557–5563, Dec. 2012.

[12] J. W. Bowen et al., ‘‘Micromachined waveguide antennas for 1.6 THz,’ Electron. Lett., vol. 42, no. 15, pp. 842–843, Jul. 2006.

[13] B. Andres-Garcia et al., ‘‘Gain enhancement by dielectric horns in the terahertz band,’’ IEEE Trans. Antennas Propag., vol. 59, no. 9, pp. 3164–3170, Sep. 2011.

[14] K. Fan, Z.-C. Hao, Q. Yuan, and W. Hong, ‘‘Development of a high gain 325–500 GHz antenna using quasi-planar reflectors,’’ IEEE Trans. Antennas Propag., vol. 65, no. 7, pp. 3384–3391, Jul. 2017.

[15] E. Lacombe et al., ‘‘Low-cost 3D-printed 240 GHz plastic lens fed by integrated antenna in organic substrate targeting sub-THz high data rate wireless links,’ in Proc. IEEE Int. Symp. Antennas Propag. USNC/URSI Nat. Radio Sci. Meeting, San Diego, CA, USA, Jul. 2017, pp. 5–6.

[16] X. Tu et al., ‘‘Diffractive microlens integrated into Nb5N6 microbolometers for THz detection,’ Opt. Exp., vol. 23, no. 11, pp. 13794–13803, Jun. 2015.
[17] H. Wang, X. Dong, M. Yi, F. Xue, Y. Liu, and G. Liu, ‘‘Terahertz highgain offset reflector antennas using SiC and CFRP material,’’ IEEE Trans. Antennas Propag., vol. 65, no. 9, pp. 4443–4451, Sep. 2017.
[18] W. Pan and W. Zeng, ‘‘Far-field characteristics of the square grooved dielectric lens antenna for the terahertz band,’ Appl. Opt., vol. 55, no. 26, pp. 7330–7336, Sep. 2016.
[19] H.-T. Zhu, Q. Xue, J.-N. Hui, and S. W. Pang, ‘‘A 750–1000 GHz Hplane dielectric horn based on silicon technology,’’ IEEE Trans. Antennas Propag., vol. 64, no. 12, pp. 5074–5083, Dec. 2016.
[20] Z.-C. Hao, J. Wang, Q. Yuan, and W. Hong, ‘‘Development of a low-cost THz metallic lens antenna,’’ IEEE Antennas Wireless Propag. Lett., vol. 16, pp. 1751–1754, 2017.
[21] T. Tajima, H.-J. Song, K. Ajito, M. Yaita, and N. Kukutsu, ‘‘300-GHz step-profiled corrugated horn antennas integrated in LTCC,’’ IEEE Trans. Antennas Propag., vol. 62, no. 11, pp. 5437–5444, Nov. 2014.
[22] Y. Liu et al., ‘‘Millimeterwave and terahertz waveguide-fed circularly polarized antipodal curvedly tapered slot antennas,’’ IEEE Trans. Antennas Propag., vol. 64, no. 5, pp. 1607–1614, May 2016.
[23] H. Lu, X. Lv, and Y. Liu, ‘‘Radiation characteristics of terahertz waveguide-fed circularly polarised antipodal exponentially tapered slot antenna,’ Electron. Lett., vol. 50, no. 16, pp. 1122–1123, Jul. 2014.
[24] K. Konstantinidis et al., ‘‘Low-THz dielectric lens antenna with integrated waveguide feed,’’ IEEE Trans. THz Sci. Technol., vol. 7, no. 5, pp. 572–581, Sep. 2017.
[25] J. Ala-Laurinaho et al., ‘‘2-D beam-steerable integrated lens antenna system for 5G E-band access and backhaul,’’ IEEE Trans. Microw. Theory Techn., vol. 64, no. 7, pp. 2244–2255, Jul. 2016.
[26] O. Yurduseven, N. L. Juan, and A. Neto, ‘‘A dual-polarized leaky lens antenna for wideband focal plane arrays,’’ IEEE Trans. Antennas Propag., vol. 64, no. 8, pp. 3330–3337, Aug. 2016.
[27] N. Llombart et al., ‘‘Silicon micromachined lens antenna for THz integrated heterodyne arrays,’’ IEEE Trans. THz Sci. Technol., vol. 3, no. 5, pp. 515–523, Sep. 2013.
[28] K. Guo, A. Standaert, and P. Reynaert, ‘‘A 525–556-GHz radiating source with a dielectric lens antenna in 28-nm CMOS,’’ IEEE Trans. THz Sci. Technol., vol. 8, no. 3, pp. 340–349, May 2018.
[29] P. Nayeri et al., ‘‘3D printed dielectric reflectarrays: Low-cost high-gain antennas at sub-millimeter waves,’’ IEEE Trans. Antennas Propag., vol. 62, no. 4, pp. 2000–2008, Apr. 2014.
[30] H. Yi, S.-W. Qu, K.-B. Ng, C. H. Chan, and X. Bai, ‘‘3-D printed millimeter-wave and terahertz lenses with fixed and frequency scanned beam,’’ IEEE Trans. Antennas Propag., vol. 64, no. 2, pp. 442–449, Feb. 2016.

[31] B. Zhang et al., ‘‘Metallic 3-D printed antennas for millimeter- and submillimeter wave applications,’’ IEEE Trans. THz Sci. Technol., vol. 6, no. 4, pp. 592–600, Jul. 2016.
[32] W. J. Otter et al., ‘‘3D printed 1.1 THz waveguides,’ Electron. Lett., vol. 53, no. 7, pp. 471–473, 2017.
[33] B. Zhang and H. Zirath, ‘‘Metallic 3-D printed rectangular waveguides for millimeter-wave applications,’’ IEEE Trans. Compon., Packag., Manuf. Technol., vol. 6, no. 5, pp. 796–804, May 2016.
[34] J. Li, T. Ma, K. Nallapan, H. Guerboukha, and M. Skorobogatiy, ‘‘3D printed hollow core terahertz Bragg waveguides with defect layers for surface sensing applications,’’ in Proc. 42nd Int. Conf. Infr., Millim. Terahertz Waves (IRMMW-THz), Cancun, Mexico, Aug./Sep. 2017, p. 1.
[35] F. Wang and T. Arslan, ‘‘Microfluidic frequency tunable three-dimensional printed antenna,’’ in Proc. IEEE MTT-S Int. Microw. Symp. Dig., Pavia, Italy, Sep. 2017, pp. 1–3.
[36] N. Chudpooti, N. Duangrit, P. Akkaraekthalin, I. D. Robertson and N. Somjit, "220-320 GHz Hemispherical Lens Antennas Using Digital Light Processed Photopolymers," in IEEE Access, vol. 7, pp. 12283-12290, 2019, doi: 10.1109/ACCESS.2019.2893230.
[37] A. E. Uya et al., "Design and Fabrication of Terahertz (THz) Antenna Using Aerosol Jet Printing," 2023 IEEE 23rd International Conference on Nanotechnology (NANO), Jeju City, Korea, Republic of, 2023, pp. 157-161, doi: 10.1109/NANO58406.2023.10231203.
[38] Optomec Marketing. (2022, April 12). *3D Printed Electronics - Aerosol Jet Technology - Optomec*. Optomec. https://optomec.com/printed-electronics/aerosol-jet-technology/
[39] Wikipedia contributors. (2022, May 16). Return loss. In *Wikipedia, The Free Encyclopedia*. Retrieved 01:27, November 6, 2023, from https://en.wikipedia.org/w/index.php?title=Return_loss&oldid=1088185680
[40] Wikipedia contributors. (2023, July 20). Insertion loss. In *Wikipedia, The Free Encyclopedia*. Retrieved 01:24, November 6, 2023, from https://en.wikipedia.org/w/index.php?title=Insertion_loss&oldid=1166201618
[41] James, J.R., Henderson, A., and HallP.S., “Microstrip Antenna Performanceis determined by Substrate Constraints,” *Microwave System News (MSN)*,August 1982, pp. 73–84.
[42] Kabacik, P., and Bialkowski, M.E., “The Temperature Dependence of Substrate Parameters and Their Effect on Microstrip Antenna Performance,”*IEEE Transactions on Antennas and Propagation*, June 1999, Vol. 47, No.6, pp. 1042–1049.
[43] Laverghetta, T.S., *Microwave Materials and Fabrication Techniques*, Third Edition, Artech House, 2000.
[44] Bancroft, R., “Conductive Ink a Match for Copper Antenna,” *Microwaves & RF*, February 1987, Vol. 26, No. 2, pp. 87–90.
[45] Vyas, R., Lakafosis, V., Rida, A., *et al*., “Paper-Based RFID-Enabled Wireless Platforms for Sensing Applications,” *IEEE Transactions on Microwave Theory and Techniques*, May 2009, Vol. 57, No. 5, pp. 1370–1382.

[46] Cruickshank, D.B., *Microwave Materials for Wireless Applications*, Artech House, 2011, pp. 44–46.
[47] Traut, G.R., "Advances in Substrate Technology," in James, J.R., and HallP.S., eds., *Handbook of Microstrip Antennas Volume 2*, Peter Peregrinus Ltd., London, 1989, Chapter 15.
[48] Howe, H., Jr., "Dielectric Material Development," *Microwave Journal*, November 1978, pp. 39–40.
[49] Bouquet, F.L., Price, W.E., and Newell, D.M., "Designer's Guide to Radiation Effects on Materials for use on Jupiter Fly-Bys and Orbiters," *IEEE Transactions on Nuclear Science*, August 1979, Vol. NS-26, No. 4, pp. 4660–4669.
[50] Rahaman, M.N., *Sintering of Ceramics*, CRC Press, 2008.
[51] Penn, S.J., Alford, N.M., Templeton, A., *et al*., "Effect of Porosity and Grain Size on the Microwave Dielectric Properties of Sintered Alumina," *Journal of American Ceramic Society*, Vol. 80, No. 7, pp. 1885–1888.
[52] Alford, N., and PennS.J., "Sintered Alumina with Low Dielectric Loss," *Journal of Applied Physics*, November 1996, Vol. 80, No. 7, pp. 5895–5898.
[53] Harper, C.A., ed., *Handbook of Plastics Technologies*, McGraw Hill, 2006, pp. 1.4–1.5.
[54] Harper, C.A., ed., *Handbook of Plastics Technologies*, McGraw Hill, 2006, pp. 3.41.
[55] Bancroft, Randy. (2009). Microstrip and Printed Antenna Design / R. Bancroft. 10.1049/SBEW048E.
[56] Wang, C., "Determining Dielectric Constant and Loss Tangent in FR-4," *UMR EMC Laboratory Technical Report: TR00-1-041*, University of Missouri, Rolla, March 2000.
[57] Wikipedia contributors. (2023, September 21). Ansys HFSS. In *Wikipedia, The Free Encyclopedia*. Retrieved 01:45, November 6, 2023, from https://en.wikipedia.org/w/index.php?title=Ansys_HFSS&oldid=1176473440